Atmospheric Pollution Research
www.atmospolres.com

Development of an extended chemical mechanism for global–through–urban applications

Prakash Karamchandani [1,2], Yang Zhang [3], Shu–Yun Chen [1,2], Rochelle Balmori–Bronson [1]

[1] *Atmospheric and Environmental Research, Inc., San Francisco, CA 94511, USA*
[2] *Currently at ENVIRON International Corporation, Novato, CA 94998, USA*
[3] *North Carolina State University, Raleigh, NC 27695, USA*

ABSTRACT

The interactions between climate and air quality are receiving increasing attention due to their high relevancy to climate change. Coupled climate and air quality models are being developed to study these interactions. These models need to address the transport and chemistry of atmospheric species over a large range of scales and atmospheric conditions. In particular, the chemistry mechanism is a key component of such models because it needs to include the relevant reactions to simulate the chemistry of the lower troposphere, the upper troposphere, and the lower stratosphere, as well as the chemistry of polluted, rural, clean, and marine environments. This paper describes the extension of an existing chemistry mechanism for urban/regional applications, the 2005 version of the Carbon Bond Mechanism (CB05), to include the relevant atmospheric chemistry for global and global–through–urban applications. Updates to the mechanism include the most important gas–phase reactions needed for the lower stratosphere as well as reactions involving mercury species, and a number of heterogeneous reactions on aerosol particles, cloud droplets, and Polar Stratospheric Clouds (PSCs). The extended mechanism, referred to as CB05 for Global Extension (CB05_GE), is tested for a range of atmospheric conditions using a zero–dimensional box–model. A comparison of results from the extended mechanism with those from the original starting mechanism for both clean and polluted conditions in the lower troposphere shows that the extended mechanism preserves the fidelity of the original mechanism under those conditions. Simulations of marine Arctic conditions, upper tropospheric conditions, and lower stratospheric conditions with the box model illustrate the importance of halogen chemistry and heterogeneous reactions (on aerosol surfaces as well as PSCs for stratospheric conditions) for predicting ozone and elemental mercury depletion events that are often observed during these conditions. Depletions that are comparable to observed depletions are predicted by the box model for very clean conditions (extremely low or zero concentrations of aldehydes and other VOCs) because, in the absence of continuous sources of active halogens, these conditions result in less conversion of active chlorine and bromine to more stable products, such as HCl and HBr.

Keywords:
Climate change and air quality
Coupled meteorological and chemistry models
Mechanism for urban through global applications
Stratospheric chemistry
Ozone and mercury depletion

Article History:
Received: 24 June 2010
Revised: 02 May 2011
Accepted: 02 May 2011

Corresponding Author:
Prakash Karamchandani
Tel: +1-415-899-0754
Fax: +1-415-899-0707
E-mail: prakash@environcorp.com
prakashk5@comcast.net

doi: 10.5094/APR.2011.047

1. Introduction

Global climate changes and air quality are closely coupled through many atmospheric meteorological, dynamic, chemical, and radiative processes. The two–way feedbacks between global climate change and urban/regional air quality requires the application of coupled climate and air quality models. The chemistry mechanism is a key component of these models because it must be applicable for a range of atmospheric conditions and must include the reactions of importance for these conditions.

Most operational atmospheric air quality models use condensed chemistry mechanisms because it is not feasible to include the entire set of atmospheric reactions and chemical species due to computational constraints. The condensation of the chemistry mechanism typically focuses on the representation in the mechanism of reactive organic gases (ROGs), also referred to as volatile organic compounds (VOCs), by combining individual VOC species using either a "lumped molecule" or "lumped structure" approach. However, the reaction set is also reduced by excluding reactions that are not of interest based on the scales or regions for which the model is designed to be applied. For example, stratospheric models (e.g., Shibata et al., 2005) employ simplified parameterizations to represent tropospheric chemistry while tropospheric models use tropopause boundary conditions or boundary conditions from global chemical transport models (CTMs) and ignore stratospheric reactions that are not important in the troposphere. For models that are or will be applied over scales ranging from urban to global, it is necessary to expand the reaction set to include all the important species and reactions of interest for a wide range of conditions. Models such as Stanford University's Gas, Aerosol, TranspOrt, Radiation, General Circulation, Mesoscale, Ocean Model (GATOR–GCMOM) (Jacobson, 2001a; Jacobson, 2001b; Jacobson, 2004) and the Lawrence Livermore National Laboratory's Integrated Massively Parallel Atmospheric Chemical Transport model (IMPACT) (Rotman et al., 2004) are two examples of such models that incorporate the reaction set necessary to simulate the chemistry of the combined troposphere and stratosphere.

The Weather Research and Forecasting/Chemistry (WRF/Chem) (Grell et al., 2005) is a community model for the regional scale that is being adapted to simulate the range of scales from global through urban (Zhang et al., 2009a; Zhang et al., 2009b). This Global–through–Urban version of WRF/Chem, referred to as GU–WRF/Chem, will provide a community tool with fully–coupled meteorology and air quality that can be used to study the interactions between climate and air quality at various scales and to support the development of emission control strategies with potential co–benefits for air quality management and climate mitigation. The latest release version of WRF/Chem (v3.2, as of April 2010) provides choices for several condensed gas–phase chemical mechanisms, including the second generation Regional Acid Deposition Model Mechanism (RADM2) (Stockwell et al., 1990), the Regional Atmospheric Chemistry Mechanism (RACM) (Stockwell et al., 1997), the Carbon Bond IV (CB–IV) mechanism (Gery et al., 1989) and the Carbon–Bond Mechanism version Z (CBM–Z) (Zaveri and Peters, 1999), a variant of CBM–IV. None of those mechanisms are suited for global or global–through–urban applications.

The CB–IV mechanism, which uses the lumped structure approach, has been widely used in urban to regional air quality modeling systems for many years. The mechanism has been extensively updated in 2005 (Yarwood et al., 2005). The updated mechanism, referred to as CB05, has now been implemented in recent versions of the Community Multiscale Air Quality model (CMAQ) (Sarwar et al., 2008) and the Comprehensive Air quality Model with extensions (CAMx), two of the most widely used urban to regional air quality modeling systems. CB05 has also been implemented into WRF/Chem (Huang et al., 2006; Pan et al., 2008).

As compared to CB–IV, CB05 includes 15 additional species and over 60 additional reactions, and updated kinetics and photolysis data, and is more suitable for simulating a wider range of conditions and species. Because of the widespread use of the Carbon–Bond mechanism in contemporary air quality models, and because CB05 already incorporates some of the additional chemistry required for long–range transport modeling and remote conditions and is also available with extensions for chlorine chemistry, as discussed in the following section, we selected CB05 as the starting point for our mechanism for global–through–urban applications. In this paper, we describe the further extension of CB05 to incorporate the species and chemistry necessary to simulate the full range of conditions required for global–through–urban modeling. We then discuss the implementation in a zero–dimensional box model of the extended CB05 mechanism, referred to as CB05 for Global Extension (CB05_GE), the subsequent testing and analysis of the mechanism for various atmospheric conditions and some qualitative comparisons to observed events such as O_3 and mercury depletion. Additional updates to the box model to incorporate aerosol and aqueous–phase chemistry treatments consistent with CB05_GE are also made but are not discussed here.

2.Extension of the CB05 mechanism for global applications

The CB05 mechanism includes updated kinetic data for the rate constant expressions, updated photolysis rate data, an extended inorganic reaction set (e.g., reactions involving H_2 and NO_3), and better representation of the atmospheric chemistry of ethane, higher aldehydes, alkenes with internal double bonds (internal olefins) (e.g., 2–butenes), oxygenated products and intermediates (e.g., higher organic peroxides and peroxycarboxylic acids), and terpenes. Yarwood et al. (2005) evaluated the CB05 mechanism using smog chamber data from the University of North Carolina, Chapel Hill, and the University of California, Riverside and found that, in general, it performed as well as or in some cases better than the CB–IV mechanism in simulating the smog chamber data. Sarwar et al. (2008) evaluated the performance of CMAQ using both the CB05 and CB–IV mechanisms and found general improvement in model performance using CB05, particularly for rural and high–altitude conditions.

The base or core CB05 mechanism has 51 species and 156 reactions (as compared to 36 species and 93 reactions in CB–IV). Optional extended versions of the core CB05 mechanism are also available; these include reactive chlorine chemistry or explicit reactions for air toxics and/or precursors to secondary organic aerosol (Yarwood et al., 2005; Sarwar et al., 2006). The CB05 mechanism with chlorine extensions for the troposphere (Sarwar et al., 2006), as implemented in CMAQ (Roselle et al., 2007) (referred to as CB05Cl) is used as a starting point for additional extension in this work. The CB05Cl mechanism consists of 177 reactions among 62 species. The chlorine component of this mechanism includes 21 reactions and 6 chlorine species.

In this work, the CB05Cl mechanism is further extended by adding reactions and species to represent mercury chemistry, the chemistry of the marine boundary layer, the chemistry of the upper troposphere and lower stratosphere, and Arctic chemistry. The resultant extended CB05 mechanism, CB05_GE, has recently been implemented into GU–WRF/Chem (Zhang et al., 2009a; Zhang et al., 2009b). An extensive literature review was conducted to identify the additional reactions and species that would be required for such extensions. The CB05_GE mechanism consists of 289 reactions among 118 species.

The updates to CB05_GE fall into the following broad categories: a) updates and additions to the halogen chemistry; b) addition of mercury chemistry; c) addition of heterogeneous reactions for global applications; d) additional reactions and species for stratospheric chemistry that are normally not included in tropospheric models; e) addition of species and reactions leading to the formation of secondary organic aerosols (SOA), and f) additional prognostic species that are normally treated as unreactive or background species with constant or stable concentrations. Examples of the latter include water vapor (H_2O), methane (CH_4), molecular oxygen (O_2), carbon dioxide (CO_2) and hydrogen (H_2). Water vapor is included to allow for feedback between the meteorological and chemistry components of WRF/Chem, while CH_4, H_2 and CO_2 are modeled species in GU–WRF/Chem with specified emission rates. O_2 is included to allow for its photolysis as a source of O_3 in the stratosphere. Note that there are some overlaps among these broad categories of updates to CB05, e.g., halogen species such as Br and BrO influence mercury chemistry and many of the additional halogen reactions are relevant to stratospheric chemistry.

Tables 1 through 5 list the extensions to CB05 for CB05_GE. Reaction rates and photolysis data are based on several sources, e.g., the latest International Union of Pure and Applied Chemistry (IUPAC) and NASA/JPL recommendations. Table 1 lists the non–halogen and non–mercury reactions that have been added to CB05_GE to represent stratospheric chemistry. These reactions include: the natural O_3 production pathway in the stratosphere via the photolysis of O_2 (i.e., the Chapman cycle; e.g., Seinfeld and Pandis, 1998; Finlayson–Pitts and Pitts, 2000; Pun et al., 2005a; Jacobson, 2005); the photolysis and reaction with the excited oxygen atom of nitrous oxide or laughing gas (N_2O), an important source of NO_x in the stratosphere and a greenhouse gas (e.g., Seinfeld and Pandis, 1998; Jacobson, 2005); the production of the hydroxyl radical (OH) by the reaction of methane with the excited oxygen atom, an important source of OH in the stratosphere (e.g., Jacobson, 2005); and the quenching of the excited oxygen atom by reaction with CO_2 (Jacobson, 2008). In addition, many of the existing CB05 reactions (not listed in Table 1) were updated to allow the explicit production of species such as H_2O and CO_2.

Table 2 shows the reaction list for the complete gas–phase halogen chemistry in CB05_GE including the CMAQ chlorine extensions (Sarwar et al., 2006; Roselle et al., 2007). The mechanism includes additional chlorine reactions for the lower

stratosphere, bromine chemistry for both the troposphere and stratosphere, and bromine/chlorine interaction reactions. As compared to CB05Cl, there are several important changes in the halogen chemistry in CB05_GE. First, the isomeric radicals, OClO and ClOO, and the chlorine monoxide dimer (also referred to as chlorine peroxide), Cl_2O_2, are included as explicit species in CB05_GE, because of their importance for stratospheric chemistry and ozone depletion (e.g., Finlayson–Pitts and Pitts, 2000). Thus, CB05_GE explicitly includes the four branches in the self–reaction of the chlorine monoxide (ClO) radical (Reactions 4 through 6 and Reaction 43 in Table 2) resulting in the production of these species, whereas CB05Cl treated them as a single reaction, yielding Cl_2 and Cl. The OClO and ClOO isomers are also by–products of the reactions of ClO with the bromine monoxide (BrO) radical (Reactions 68 through 70). Second, CB05_GE accounts for the release of chlorine atoms from the reservoir species, hydrogen chloride (HCl), via photolysis (Reaction 23) and reaction with the hydroxyl radical (Reaction 36). While these reactions are relatively slow compared to the heterogeneous reactions of HCl and other reservoir species on Polar Stratospheric Clouds (PSCs), they are included for completeness following Rotman et al. (2004). Third, Reaction 29 is included to complete the rapid chlorine oxides (ClO_x) cycle of O_3 destruction involving the chlorine monoxide (ClO) radical (e.g., Seinfeld and Pandis, 1998; Finlayson–Pitts and Pitts, 2000). Fourth, the reaction of OH with ClO (Reaction 30) is included, which primarily produces HO_2 and Cl, but also creates a small amount of the reservoir species, HCl (Finlayson–Pitts and Pitts, 2000). Fifth, the reactions of the chlorine atom with the hydroperoxy (HO_2) radical (Reactions 31 and 32) are included to create the reservoir species, HCl and ClO; and the reactions of Cl with hydrogen and hydrogen peroxide (Reactions 41 and 42) and (H_2O_2) to form HCl are also included following Rotman et al. (2004). Sixth, the photolysis reactions of the chlorofluorocarbon species, $CFCl_3$ (CFC–11) and CF_2Cl_2 (CFC–12) are added to generate chlorine atoms (Reactions 37 and 38). Seventh, the photolysis of methyl chloride (CH_3Cl) and its reaction with OH to generate chlorine atoms (Reactions 39 and 40) are included. Finally, bromine reactions (Reactions 49 through 78) are included in CB05_GE to represent the chemistry of bromine in the troposphere (e.g., von Glasow et al., 2004; Yang et al., 2005) and stratosphere (e.g., Seinfeld and Pandis, 1998; Finlayson–Pitts and Pitts, 2000; Rotman et al., 2004; Jacobson, 2005) including chlorine–bromine interaction reactions, photolysis of halons (Halon 1211 or CF_2ClBr and Halon 1301 or CF_3Br) and methyl bromide, and reaction of methyl bromide with OH. Note that many of the bromine reactions are analogous to the chlorine reactions.

Table 1. *Non–halogen gas–phase stratospheric reactions in the CB05_GE mechanism*

No.	Reactants[a]	Products[a]	Rate Expression[b]
1	O_2	2O	Photolysis
2	$O + O_3$	$2O_2$	$8.70 \times 10^{-12}\ e^{(-2060/T)}$
3	N_2O	$O(^1D)$	Photolysis
4	$N_2O + O(^1D)$[c]	1.24NO	1.16×10^{-10}
5	$CH_4 + O(^1D)$[c]	0.9MEO2 + 0.9OH + 0.1FORM + 0.1H_2	1.55×10^{-10}
6	$CO_2 + O(^1D)$	$O + CO_2$	$7.5 \times 10^{-11}\ e^{(115/T)}$

[a] *MEO2: methyl peroxy radical; FORM: formaldehyde.*
[b] *First-order rate constants are in units of sec^{-1}, second-order rate constants are in units of cm^3 $molecules^{-1}$ sec^{-1} and temperatures (T) are in Kelvin.*
[c] *Composite reaction representing multiple branches.*

For the global model simulations with CB05_GE, the emissions of the stratospheric halogen source gases (CFCs, halons, methyl chloride) are based on data from the Intergovernmental Panel on Climate Change (IPCC, 2001), REanalysis of the TROpospheric chemical composition (RETRO; Schultz et al., 2007) and the Reactive Chlorine Emissions Inventory (RCEI; Graedel and Keene, 1999 and references therein, including Keene et al., 1999).

Table 2. *Gas–phase halogen reactions in the CB05_GE mechanism*

No.	Reactants[a]	Products[a]	Rate Expression[b]
1	Cl_2	2Cl	Photolysis
2	HOCl	OH + Cl	Photolysis
3	$Cl + O_3$	ClO	$2.3 \times 10^{-11}\ e^{(-200/T)}$
4	ClO + ClO	Cl_2	$1.0 \times 10^{-12}\ e^{(-1590/T)}$
5	ClO + ClO	Cl + ClOO	$3.0 \times 10^{-11}\ e^{(-2450/T)}$
6	ClO + ClO	Cl + OClO	$3.5 \times 10^{-13}\ e^{(-1370/T)}$
7	ClO + NO	$Cl + NO_2$	$6.4 \times 10^{-12}\ e^{(290/T)}$
8	$ClO + HO_2$	HOCl	$2.7 \times 10^{-12}\ e^{(220/T)}$
9	OH + FMCL	$Cl + CO + H_2O$	5.00×10^{-13}
10	FMCL	$Cl + CO + HO_2$	Photolysis
11	$Cl + CH_4$	HCl + MEO2	$6.6 \times 10^{-12}\ e^{(-1240/T)}$
12	Cl + PAR	Multiple products	5.00×10^{-11}
13	Cl + ETHA	Multiple products	$8.3 \times 10^{-11}\ e^{(-100/T)}$
14	Cl + ETH	FMCL + $2XO_2$ + HO_2 + FORM	1.07×10^{-10}
15	Cl + OLE	Multiple products	2.5×10^{-10}
16	Cl + IOLE	Multiple products	3.5×10^{-10}
17	Cl + ISOP	Multiple products	4.3×10^{-10}
18	Cl + FORM	$HCl + HO_2 + CO$	$8.2 \times 10^{-11}\ e^{(-34/T)}$
19	Cl + ALD2	HCl + C2O3	7.9×10^{-11}
20	Cl + ALDX	HCl + CXO3	1.3×10^{-10}
21	Cl + MEOH	$HCl + HO_2$ + FORM	5.5×10^{-11}
22	Cl + ETOH	$HCl + HO_2$ + ALD2	$8.2 \times 10^{-11}\ e^{(45/T)}$
23	HCl + OH	$Cl + H_2O$	$6.58 \times 10^{-13}\ (T/300)^{1.16}\ e^{(58/T)}$
24	$ClO + NO_2$	$ClONO_2$	Falloff[c] $k_0 = 1.6 \times 10^{-31}\ (T/300)^{-3.4}$ $k_\infty = 7.0 \times 10^{-11}$ $F = 0.4$
25	$ClONO_2$	$ClO + NO_2$	Photolysis
26	$ClONO_2$	$Cl + NO_3$	Photolysis
27	$Cl + NO_2$	$ClNO_2$	Falloff[c] $k_0 = 1.8 \times 10^{-31}\ (T/300)^{-2.0}$ $k_\infty = 1.0 \times 10^{-10}\ (T/300)^{-1.0}$ $F = 0.6$
28	$ClNO_2$	$Cl + NO_2$	Photolysis
29	ClO + O	Cl	$2.5 \times 10^{-11}\ e^{(110/T)}$
30	ClO + OHc	$0.94Cl + 0.94HO_2$ + 0.06HCl	2.0×10^{-11}
31	$Cl + HO_2$	HCl	3.4×10^{-11}
32	$Cl + HO_2$	ClO + OH	$6.3 \times 10^{-11}\ e^{(-570/T)}$
33	OClO	ClO + O	Photolysis
34	Cl + OClO	2ClO	$3.2 \times 10^{-11}\ e^{(170/T)}$
35	OH + OClO	HOCl	$1.4 \times 10^{-12}\ e^{(600/T)}$
36	HCl	$Cl + HO_2$	Photolysis
37	$CFCl_3$	3Cl	Photolysis
38	CF_2Cl_2	2Cl	Photolysis
39	CH_3Cl	MEO2 + Cl	Photolysis
40	$OH + CH_3Cl$	$Cl + H_2O$	$2.4 \times 10^{-12}\ e^{(-1250/T)}$
41	$Cl + H_2$	$HCl + HO_2$	$3.9 \times 10^{-11}\ e^{(-2310/T)}$
42	$Cl + H_2O_2$	$HCl + HO_2$	$1.1 \times 10^{-11}\ e^{(-980/T)}$
43	ClO + ClO	Cl_2O_2	Falloff[d] $k_0 = 2.0 \times 10^{-32}\ (T/300)^{-4.0}$ $k_\infty = 1.0 \times 10^{-11}$ F = 0.45
44	Cl2O2	Cl + ClOO	Photolysis
45	ClOO + M	Cl + M	$2.8 \times 10\text{-}10\ e^{(-1820/T)}$
46	ClOO + Cl[c]	$0.95Cl_2$ + 0.1ClO	2.4×10^{-10}
47	$Cl + NO_3$	$ClO + NO_2$	2.4×10^{-11}
48	OH + HOCl	$ClO + H_2O$	5.0×10^{-13}
49	Br_2	2Br	Photolysis
50	HOBr	OH + Br	Photolysis
51	$Br + O_3$	BrO	$1.7 \times 10^{-11}\ e^{(-800/T)}$
52	BrO + BrO	Br_2	$2.9 \times 10^{-14}\ e^{(840/T)}$
53	BrO + BrO	2Br	2.7×10^{-12}
54	BrO + NO	$Br + NO_2$	$8.7 \times 10^{-12}\ e^{(260/T)}$
55	$BrO + HO_2$	HOBr	$4.5 \times 10^{-12}\ e^{(500/T)}$

Table 2. *Gas–phase halogen reactions in the CB05_GE mechanism (continued)*

No.	Reactants[a]	Products[a]	Rate Expression[b]
56	Br + FORM	$HBr + HO_2 + CO$	$7.7 \times 10^{-12}\ e^{(-580/T)}$
57	Br + ALD2	HBr + C2O3	$1.8 \times 10^{-11}\ e^{(-460/T)}$
58	HBr + OH	$Br + H_2O$	$6.7 \times 10^{-12}\ e^{(155/T)}$
59	$BrO + NO_2$	$BrONO_2$	Falloffd $k_0 = 4.7 \times 10^{-31}\ (T/300)^{-3.1}$ $k_\infty = 1.8 \times 10^{-11}$ F = 0.4
60	$BrONO_2$	$BrO + NO_2$	Photolysis
61	$BrONO_2$	$Br + NO_3$	Photolysis
62	BrO + O	Br	$1.9 \times 10^{-11}\ e^{(230/T)}$
63	BrO + OH	$Br + HO_2$	$1.8 \times 10^{-11}\ e^{(250/T)}$
64	$Br + HO_2$	HBr	$7.7 \times 10^{-12}\ e^{(-450/T)}$
65	$Br + NO_2$	$BrNO_2$	Falloffd $k_0 = 4.2 \times 10^{-31}\ (T/300)^{-2.4}$ $k_\infty = 2.7 \times 10^{-11}$ F = 0.55
66	$BrNO_2$	$Br + NO_2$	Photolysis
67	BrO	Br + O	Photolysis
68	BrO + ClO	Br + OClO	$1.6 \times 10^{-12}\ e^{(430/T)}$
69	BrO + ClO	Br + ClOO	$2.9 \times 10^{-12}\ e^{(220/T)}$
70	BrO + ClO	BrCl	$5.8 \times 10^{-13}\ e^{(170/T)}$
71	BrCl	Br + Cl	Photolysis
72	HOBr + O	OH + BrO	$1.2 \times 10^{-10}\ e^{(-430/T)}$
73	Br_2 + OH	HOBr + Br	$2.0 \times 10^{-11}\ e^{(240/T)}$
74	HBr	$Br + HO_2$	Photolysis
75	CF_2ClBr	Cl + Br	Photolysis
76	CF_3Br	Br	Photolysis
77	CH_3Br	MEO2 + Br	Photolysis
78	OH + CH_3Br	$Br + H_2O$	$2.35 \times 10^{-12}\ e^{(-1300/T)}$

[a] *FMCL: formyl chloride; PAR, ETHA, ETH, OLE, IOLE, ISOP, ALD2, ALDX, MEOH, ETOH: paraffin carbon bond, ethane, ethane, terminal olefin bond, internal olefin bond, isoprene, acetaldehyde, propionaldehyde and higher aldehydes, methanol, ethanol; XO2, C2O3, CXO3: NO to NO_2 conversion from alkylperoxy radical, acetylperoxy radical, C3 and higher acylperoxy radicals.*

[b] *First-order rate constants are in units of sec^{-1}, second-order rate constants are in units of cm^3 $molecules^{-1}$ sec^{-1} and temperatures (T) are in Kelvin.*

[c] *Composite reaction representing multiple branches*

[d] *The rate constant is* $k = \left[\frac{k_o[M]}{1+k_0[M]/k_\infty}\right] F^Z$ *, where [M] is the total pressure in molecules cm^{-3} and* $Z = \left\{1 + \left(log_{10}\frac{k_0[M]}{k_\infty}\right)^2\right\}^{-1}$

The mercury reactions added to the CB05_GE gas–phase chemistry mechanism are listed in Table 3. Mercury (Hg) is an important pollutant at all scales ranging from global to local. The chemistry of Hg plays an important role in both the cycling of Hg and its atmospheric residence time, and the deposition and bioaccumulation of Hg with its associated health effects. Mercury exists in the atmosphere as elemental mercury, Hg(0), and oxidized (divalent) mercury, Hg(2) (Schroeder and Munthe, 1998). Hg(2) can be inorganic (e.g., mercuric chloride, $HgCl_2$) or organic (e.g., methyl mercury, MeHg). It can also be present as particulate mercury (e.g., mercuric oxide, HgO, or mercury sulfide, HgS). In the global atmosphere, Hg(0) is the dominant form. Hg(2) typically constitutes a few percent of total mercury and is predominantly in the gas phase. MeHg concentrations in the atmosphere are negligible; however, Hg(2) becomes methylated in water bodies where it can bioaccumulate in the food chain. Hg(0) is sparingly soluble and is not removed significantly by wet deposition; its dry deposition velocity is also believed to be low. As a result, Hg(0) has a long atmospheric lifetime, on the order of several months to more than a year (e.g., Lindberg et al., 2007), that is governed by its oxidation to Hg(2). On the other hand, Hg(2) is quite soluble; it is consequently removed rapidly by wet and dry deposition processes. Particulate mercury, Hg(p), is present in the fine fraction of particulate matter ($PM_{2.5}$), although some Hg(p) may be present in coarse particulate matter (PM) (Bullock and Brehme, 2002).

Table 3. *Gas-phase mercury reactions in the CB05_GE mechanism*

No.	Reactants	Products	Rate Expression[a]
1	$Hg(0) + O_3$	Hg(2)	3.0×10^{-20}
2	Hg(0) + OH	Hg(2)	8.7×10^{-14}
3	$Hg(0) + H_2O_2$	Hg(2)	8.5×10^{-19}
4	Hg(0) + (Br, BrO)	Hg(2)	Special[b]

[a] *First-order rate constants are in units of sec^{-1} and second-order rate constants are in units of cm^3 $molecule^{-1}$ sec^{-1}.*

[b] *Special reaction representing the following set of reactions:*

1. *Hg(0) + Br → HgBr, $k_1 = 3.6 \times 10^{-13}\ P\ (T/298)^{-1.86}$ cm^3 $molecules^{-1}$ sec^{-1}*
2. *HgBr → Hg(0), $k_2 = 3.9 \times 10^9\ e^{(-8357/T)}$ sec^{-1}*
3. *HgBr + Br → $HgBr_2$, $k_3 = 2.5 \times 10^{-10}\ (T/298)^{-0.57}$ cm^3 $molecules^{-1}$ sec^{-1}*
4. *HgBr + OH → HgBrOH, $k_4 = 2.5 \times 10^{-10}\ (T/298)^{-0.57}$ cm^3 $molecules^{-1}$ sec^{-1}*
5. *Hg(0) + BrO → Hg(2), $k_5 = 1 \times 10^{-15}$ cm^3 $molecules^{-1}$ sec^{-1}*

In the above rate expressions, P is the pressure in atmospheres and T is the temperature in Kelvin.

Assuming that Br, BrO and OH concentrations are negligibly perturbed by their reactions with mercury, an effective Hg(0) first-order rate constant can be calculated as follows:

$$k_{eff} = \frac{k_1[Br]\left(k_3[Br] + k_4[OH]\right)}{k_2 + k_3[Br] + k_4[OH]} + k_5[BrO]\ \ sec^{-1},$$

where [Br], [OH] and [BrO] are the concentrations of Br, OH, and BrO in molecules cm^{-3}, respectively.

Known transformations among inorganic mercury species include the gas–phase oxidation of Hg(0) to Hg(2), the aqueous–phase oxidation of Hg(0) to Hg(2), the aqueous–phase reduction of Hg(2) to Hg(0), various aqueous–phase equilibria of Hg(2) species and the aqueous–phase adsorption of Hg(2) to PM. The CB05_GE mechanism includes the gas–phase reactions and the box model used to test the mechanism includes the various aqueous–phase processes. There are, however, some uncertainties in the kinetics and mechanisms of some of those reactions (Calvert and Lindberg, 2005; Lin et al., 2006; Seigneur et al., 2006). Until recently, most models for mercury chemistry have been based on the assumption that OH and O_3 are the primary gas–phase oxidants for Hg(0). However, there is evidence to suggest that halogen species such as bromine and chlorine can play an important role in converting elemental mercury to divalent mercury. Bromine species are responsible for mercury depletion events (MDEs) in the Arctic (Schroeder et al., 1998; Lindberg et al., 2002) and Antarctic (Ebinghaus et al., 2002; Temme et al., 2003), where Hg(0) is rapidly oxidized to Hg(2), which subsequently is deposited to the ground. In addition, bromine may also convert Hg(0) to Hg(2) in the marine boundary layer thereby leading to rapid deposition of some Hg to the ocean (Mason and Sheu, 2002) and possibly near the tropopause where high concentrations of particulate Hg (most likely adsorbed Hg(2)) have been observed (Murphy and Thomson, 2000; Murphy et al., 2006). The chemical kinetics of halogen reactions with Hg(0) indicates that the major reactions are the oxidation of Hg(0) by bromine atoms (Br) and BrO radicals (Ariya et al., 2002; Ariya et al., 2004).

The gas–phase mercury chemistry mechanism in CB05_GE, shown in Table 3, consists of the following reactions: the oxidation of Hg(0) to Hg(2) by O_3 (Hall, 1995), hydrogen peroxide (Tokos et al., 1998), OH (Sommar et al., 2001; Pal and Ariya, 2003; Pal and Ariya, 2004), Br (Ariya et al., 2002), and BrO (Raofie and Ariya, 2003). The oxidation of Hg(0) by Br and BrO in CB05_GE is based on a sequence of 5 reactions (Seigneur and Lohman, 2008). The 5 reactions are treated as a single reaction, with an effective Hg(0) first–order rate constant that is a function of the individual reaction rates and the concentrations of Br, BrO and OH (see the footnote in Table 3). This treatment is similar to that of Holmes et al. (2006), who considered the oxidation of Hg(0) by bromine atoms with a set of 3 reactions.

The role of iodine chemistry in ozone and mercury depletion has also been investigated in several studies (e.g., Davis et al., 1996; Vogt et al., 1999; Calvert and Lindberg, 2004a; Calvert and Lindberg, 2004b). Under certain conditions in the marine boundary layer (e.g., Huang et al., 2010) or in the Antarctic atmosphere (e.g., Friess et al., 2010), iodine compounds may be present in sufficient amounts to influence the chemistry. However, there are significant uncertainties in iodine chemistry as well as the sources of marine iodine (e.g., Davis et al., 1996) and iodine levels are usually below detection limits in other environments, such as the Arctic (e.g., Pohler et al., 2010). Thus, we have not included iodine chemistry in the CB05_GE mechanism at this time, but future versions of the mechanism may include it if appropriate information is available.

Table 4 lists the reactions added to CB05_GE to represent the formation of SOA precursors that are consistent with the SOA treatment in the Model of Aerosol Dynamics, Reaction, Ionization and Dissolution (MADRID) of Zhang et al. (2004) and its updated version (Zhang et al., 2010), based on recent updates to MADRID by Pun et al. (2005b). The updated mechanism includes the formation of 25 SOA species from four anthropogenic precursor gases [two aromatic compounds represented by toluene and xylene, and long–chain alkanes and polycyclic aromatic hydrocarbon (PAH) species], and 7 biogenic precursor gases (isoprene, five monoterpenes, and sesquiterpene). The formation of SOA from isoprene is based on Henze and Seinfeld (2006), Kroll et al. (2006), and Zhang et al. (2007).

It should be noted that Archibald et al. (2010a) used a 0–D box model to intercompare the isoprene chemistry in a number of mechanisms incorporated in current CTMs, including the CB05 mechanism used as the foundation of the global–through–urban mechanism described here. The isoprene chemistry portion of these mechanisms ranged in size and complexity from 12 species and 24 reactions for the simplest mechanism (STOCHEM) to nearly 180 species and 600 reactions for the detailed mechanism (MCMv3.1). In comparison, the CB05 isoprene chemistry mechanism consisted of 17 species and 49 reactions. Archibald et al. (2010a) found that none of the mechanisms were able to generate/recycle HO_x at the rates needed to match observed levels of OH concentrations in isoprene–rich low–NO_x environments, such as over the Amazonian rainforest (e.g., Lelieveld et al., 2008; Martinez et al., 2010) and the tropical forests of Borneo (e.g., Pugh et al., 2010a), Ren et al. (2008) noted similar inconsistencies between model estimates and observed levels of OH concentrations during the Intercontinental Chemical Transport Experiment–A (INTEX–A) over forested regions of the United States where isoprene is abundant, primarily from the Gulf Coast states up through Appalachia and the Midwest. They found that OH concentrations were underestimated by a factor of five or more when isoprene concentrations exceeded 500 pptv.

From these and other similar studies, there is general agreement that current models and mechanisms are missing an important pathway to generate/recycle HO_x under high isoprene and low NO_x conditions. However, there are several uncertainties with regard to the exact nature of this pathway and how to represent it. For example, some models artificially address this issue by reducing the strength of the isoprene source by a factor of two or more. As pointed out by Lelieveld et al. (2008), this may achieve the desired effect of increasing simulated OH levels but hampers the understanding of the atmospheric processes involved and may possibly result in other model errors. Lelieveld et al. (2008) forced their isoprene mechanism to recycle 40–80% of the OH by prescribing OH yields from reactions between HO_2 and organic peroxy radicals to achieve better agreement with observed OH levels. A similar approach was taken by Butler et al. (2008) and Kubistin et al. (2010), who artificially added OH to the products of the reactions between HO_2 and isoprene–derived organic peroxy radicals. Other chemical pathways that lead to increases in OH concentrations under low NO_x conditions in isoprene–rich environments have been postulated by Paulot et al. (2009) and Peeters et al. (2009). The latter proposed the inclusion of uni–molecular isomerizations of the isoprene hydroxy–peroxy radicals leading to enhanced production of HO_x radicals and ozone (Peeters et al., 2009; Peeters and Muller, 2010) and Stavrokou et al. (2010) found that this pathway resulted in better agreement of observed and modeled OH levels.

Table 4. *SOA precursor reactions in the CB05_GE mechanism*

No.	Reactants[a]	Products[a,b]	Rate Expression [c]
1	TOL + OH	0.44 HO_2 + 0.08 XO2 + 0.36 CRES + 0.56 TO2 + 0.071 TOLAER1 + 0.138 TOLAER2	$1.8 \times 10^{-12}\ e^{(355/T)}$
2	XYL + OH	0.70 HO_2 + 0.50 XO2+ 0.20 CRES + 0.80 MGLY + 1.10 PAR + 0.30 TO2 + 0.038 XYLAER1+ 0.167 XYLAER2	$1.7 \times 10^{-11}\ e^{(116/T)}$
3	ISOP + O	0.75 ISPD + 0.50 FORM + 0.25 XO2 + 0.25 HO_2 + 0.25 CXO3 + 0.25 PAR + 0.232 ISOAER1+ 0.0288 ISOAER2	3.6×10^{-11}
4	ISOP + OH	0.912 ISPD + 0.629 FORM + 0.991 XO2 + 0.912 HO_2 + 0.088 XO2N + 0.232 ISOAER1 + 0.0288 ISOAER2	$2.54 \times 10^{-12}\ e^{(407.6/T)}$
5	ISOP + O_3	0.650 ISPD + 0.600 FORM + 0.200 XO2 + 0.066 HO_2 + 0.266 OH + 0.200 CXO3 + 0.150 ALDX + 0.350 PAR + 0.066 CO + 0.068 CO_2 + 0.232 ISOAER1 + 0.0288 ISOAER2	$7.86 \times 10^{-15}\ e^{(-1912/T)}$
6	ISOP + NO_3	0.200 ISPD + 0.800 NTR + XO2 + 0.800 HO_2 + 0.200 NO_2 + 0.800 ALDX + 2.400 PAR + 0.232 ISOAER1+ 0.0288 ISOAER2	$3.03 \times 10^{-12}\ e^{(-448/T)}$
7	HUM + OH	HUMAER + OH	2.93×10^{-10}
8	LIM + OH	0.239 LIMAER1 + 0.363 LIMAER2 + OH	1.71×10^{-10}
9	OCI + OH	0.045 OCIAER1+ 0.149 OCIAER2 + OH	2.52×10^{-10}
10	APIN + OH	0.038 APINAER1+ 0.326 APINAER2 + OH	5.37×10^{-11}
11	APIN + O_3	0.125 APINAER3 + 0.102 APINAER4 + O_3	8.66×10^{-17}
12	BPIN + OH	0.13 BPINAER1+ 0.0406 BPINAER2 + OH	7.89×10^{-11}
13	BPIN + O_3	0.026 BPINAER3 + 0.485 BPINAER4 + OH	1.36×10^{-17}
14	BPIN + NO_3	BPINAER5 + NO_3	2.31×10^{-12}
15	TER + OH	0.091 TERAER1 + 0.367 TERAER2 + OH	2.7×10^{-10}
16	ALKH + OH	1.173 ALKHAER1 + OH	1.97×10^{-11}
17	PAH + OH	0.156 PAHAER1 + 0.777 PAHAER2 + OH	7.7×10^{-11}

[a] TOL, XYL: toluene and other monoalkyl aromatics, xylene and other polyalkyl aromatics; HUM, LIM, OCI, APIN, BPIN, TER: humulene, limonene, ocimine, α-pinene, β-pinene, terpinene; ALKH, PAH: long-chain alkanes, polycyclic aromatic hydrocarbons; CRES, MGLY, ISPD, NTR: cresol and higher molecular weight phenols, methylglyoxal and other aromatic products, isoprene product (lumped methacrolein, methyl vinyl ketone, etc.), organic nitrate; TO2, XO2N: toluene-hydroxyl radical adduct, NO to organic nitrate conversion from alkylperoxy radical; xxxAERn: SOA products where xxx is the precursor and n is an integer.

[b] The oxidants (e.g., OH, O_3, and NO_3) are assumed to be unaffected by each reaction following the approach of Zhang et al. (2004).

[c] Second-order rate constants are in units of cm^3 $molecule^{-1}$ sec^{-1}.

Pugh et al. (2010a) have suggested that increasing OH production artificially may adversely affect the model fit for VOCs and those shortcomings in the representation of both chemistry and dynamics must be addressed to reconcile the discrepancies between observed and simulated OH levels. They found that reducing the isoprene+OH rate constant by 50% (to account for air mass segregation effects for OH and isoprene, also proposed by Butler et al., 2008), in conjunction with increased deposition of intermediates and some modest OH recycling, was able to produce levels of both isoprene and OH concentrations that were in reasonable agreement with observed values. However, a more recent study by the same authors (Pugh et al., 2010b) indicates that the effects of segregation may be substantially smaller (about 15% reduction in the rate constant of the isoprene+OH reaction) than the 50% reduction previously reported, in agreement with the 15% phenomenological reduction in rate coefficient reported by Dlugi et al. (2010), based on measurements over a deciduous forest in Germany.

Archibald et al. (2010b) recently conducted several sensitivity studies using a simple box model to investigate the impacts of the alternative approaches discussed above, such as OH propagating channels from the reaction of HO_2 with isoprene–derived organic peroxy radicals, and the chemical pathways postulated by Paulot et al. (2009) and Peeters et al. (2009). They found that the highest potential impacts (up to a factor of 3 increase in simulated OH concentrations) were obtained by implementing the isomerization reactions proposed by Peeters et al. (2009). However, they also found that the modified mechanism could not be fully reconciled with other atmospheric observations and existing laboratory data (such as the results of Paulot et al., 2009) without some degree of parameter refinement and optimization and recommended additional studies to validate the proposed mechanism. The effects of the isomerization updates to the isoprene mechanism were also subsequently tested by Archibald et al. (2011) using a global chemistry–climate model. While they noted large increases in modeled OH concentrations with the chemistry updates, they reiterated their recommendations to conduct additional studies to validate the mechanism and refine the parameters. More recently, Zhang et al. (2011), added a HO_x recycling scheme based upon Peeters et al. (2009) to MCM v3.1 and the CB05 mechanisms, and found that the Peeters et al. (2009) isoprene chemistry tended to significantly over–predict observed chamber O_3 concentrations. They also suggest that more low–NO_x experiments and further confirmation of current theoretical studies are needed. Another recent study by Whalley et al. (2011) also suggests that additional novel OH source mechanisms and HO_2 sink mechanisms are needed to fully reconcile recent radical measurements in a Borneo rainforest.

Because of these uncertainties and the ongoing research to develop a generalized isoprene chemistry mechanism, our current CB05_GE mechanism does not incorporate these updates to the isoprene chemistry. Nevertheless, we note that this is an area of future improvement to the mechanism, like the role of iodine chemistry in ozone and mercury depletion, discussed previously.

Table 5 lists the heterogeneous reactions included in CB05_GE. These reactions include heterogeneous reactions on aerosol surfaces, cloud droplets and polar stratospheric clouds (PSCs). These reactions are necessary to explain observed stratospheric O_3 depletion events as well as surface ozone and elemental mercury depletion events during the polar spring in the Antarctic and the Arctic (e.g., Schroeder et al., 1998; Foster et al., 2001; Bottenheim et al., 2002a; Lindberg et al., 2002; Spicer et al., 2002; Skov et al., 2004). These reactions convert chlorine and bromine reservoir species (such as HCl, HBr, $ClONO_2$ and $BrONO_2$) into the more reactive forms (e.g., Cl_2, Cl, Br_2, Br, ClO, BrO, BrCl). For example, von Glasow et al. (2004) have noted that the cycling of HOBr, HBr and $BrONO_2$ is very slow when only gas–phase reactions are included, and it is necessary to include heterogeneous reactions on the surfaces of aerosol particles and sea–ice particles to cycle the reactive bromine and chlorine. PSCs, that exist in the lower stratosphere at altitudes between 15 km and 25 km, provide yet another medium for this heterogeneous conversion (e.g., Lary et al., 1996; Tie and Brasseur, 1996).

Table 5a. *Heterogeneous reactions on aerosol particles in the CB05_GE mechanism*

No.	Reactants	Products	Reaction Probability
1	HO_2	$0.5H_2O_2$	0.2
2	NO_2	$0.5HONO + 0.5HNO_3$	0.
3	$NO_3 + H_2O$	$HNO_3 + OH$	1.0×10^{-3}
4	$N_2O_5 + H_2O$	$2HNO_3$	0.1
5	$ClONO_2 + H_2O$	$HOCl + HNO_3$	0.001[a], 0.01[b]
6	$ClONO_2 + HCl$	$Cl_2 + HNO_3$	0.0001[a], 0.01[b]
7	$HOCl + HCl$	$Cl_2 + H_2O$	0.001[a], 0.1[b]
8	$BrONO_2 + H_2O$	$HOBr + HNO_3$	0.03[a], 0.8[b]
9	$BrONO_2 + HCl$	$BrCl + HNO_3$	0.00001[a], 0.8[b]
10	$HOBr + HCl$	$BrCl + H_2O$	0.0001[a], 0.2[b]
11	$HOBr + HBr$	$Br_2 + H_2O$	0.0001[a], 0.25[b]
12	$SO_2 + O_3$	H_2SO_4	0.0003

[a] *Reaction probability for moderate temperatures*
[b] *Reaction probability for cold temperatures or stratosphere*

Table 5b. *Heterogeneous reactions on cloud droplets in the CB05_GE mechanism*

No.	Reactants	Products	Reaction Probability
1	HO_2	$0.5H_2O_2$	0.2
2	$NO_3 + H_2O$	$HNO_3 + OH$	1.0×10^{-3}

Table 5c. *Heterogeneous reactions on Polar Stratospheric Clouds (PSCs) in the CB05_GE mechanism*

No.	Reactants	Products	Reaction Probability
1	$ClONO_2 + H_2O$	$HOCl + HNO_3$	0.004[a], 0.3[b]
2	$ClONO_2 + HCl$	$Cl_2 + HNO_3$	0.2[a], 0.3[b]
3	$HOCl + HCl$	$Cl_2 + H_2O$	0.1[a], 0.2[b]
4	$N_2O_5 + H_2O$	$2HNO_3$	0.0004[a], 0.2[b]
5	$N_2O_5 + HCl$	$ClNO_2 + HNO_3$	0.003[a], 0.03[b]
6	$BrONO_2 + H_2O$	$HOBr + HNO_3$	0.2
7	$BrONO_2 + HCl$	$BrCl + HNO_3$	0.3
8	$HOBr + HCl$	$BrCl + H_2O$	0.3
9	$HOBr + HBr$	$Br_2 + H_2O$	0.1
10	$ClONO_2 + HBr$	$BrCl + HNO_3$	0.3

[a] *Reaction probability for Type I PSCs*
[b] *Reaction probability for Type II PSCs*

The heterogeneous reactions include 12 reactions on particle surfaces (Table 5a), including the oxidation of SO_2 to sulfate on mineral aerosols based on Dentener et al. (1996); 2 reactions on cloud droplets (Table 5b); and 10 reactions on Type I and Type II PSCs (Table 5c). The chemistry is assumed to occur between a gas–phase species and an adsorbed species. Following Jacob (2000), reaction probabilities are used to derive first–order rate constants for heterogeneous loss of the gas–phase species to the adsorbing surface. The rate constants are functions of the total surface area concentration of particles, the reaction probability (also called the uptake coefficient) of the gas, and the thermal speed of the impinging gas (e.g., Jacobson, 2005). Second–order reaction rate constants are then determined for most of the reactions by dividing the first–order rate constants by the concentration of the adsorbed species. This allows the calculation of the loss of the adsorbed species. This approach is similar to that used in the Modular Earth Submodel System (MESSy) developed at the Max Planck Institute for Chemistry in Mainz, Germany (Jockel et al., 2005; Jockel et al., 2006). For a few reactions, where there is an excess of the adsorbed reactant, it is sufficient to use the first–order rate for the gas–phase species.

Reaction probabilities for most of the reactions in Table 5 are based on literature values where available (e.g., Jacob, 2000; Finlayson–Pitts and Pitts, 2000; Jacobson, 2005; Sander et al., 2006). It should be noted that there are large uncertainties in many of the reaction probabilities and they should be considered as order of magnitude estimates. For reactions on aerosol particles, we assume different reaction probabilities for typical tropospheric ambient conditions versus very cold stratospheric conditions. This distinction is made based on the observation that heterogeneous halogen activation is very efficient under cold or stratospheric conditions as compared to moderate temperatures (e.g., Engel et al., 2000; Tarasick and Bottenheim, 2002).

Because the extensions in the CB05_GE mechanism result in an increase in both the number of species and the number of reactions, it is useful to determine the computational penalty associated with the extensions. In the box–model simulations described in the following section, we found that CPU times for CB05_GE were 15 to 20% higher than those for CB05Cl. These simulations consider chemistry only. In a global–through–urban CTM simulation, there will be additional computational penalties associated with the extra CB05_GE species transported in the model. Nevertheless, the chemistry computational penalty is a good indicator of the overall computational penalty, since a majority of the CPU cycles in a CTM simulation are spent in the chemistry solver. We estimate the overall computational penalty with CB05_GE to be in the range of 30 to 40%. Given the powerful computers available today with multi–processing capabilities, this is an acceptable penalty in exchange for the ability to simulate a large range of scales in one model application.

3. Box–Model Results with CB05_GE

In order to test the extended CB05_GE mechanism, we conducted several sets of box–model simulations. We first compared model results with those from the original CB05 mechanism with chlorine extensions (CB05Cl) for both rural (clean) and urban (polluted) conditions in the lower troposphere. The objective of this exercise was to ensure that the extensions to the CB05Cl mechanism, which were primarily included to make the mechanism suitable for global applications, had a small effect in urban or regional tropospheric conditions where the additional reactions would be unimportant or play a minor role. Subsequent testing of the CB05_GE mechanism focused on its ability to qualitatively reproduce some of the observed features of the chemistry at higher altitudes and in the marine Arctic. Below, we discuss these simulations and some important findings.

3.1. Comparison with CB05Cl mechanism

The CB05_GE mechanism development described here is somewhat different from typical air quality model chemical mechanism development studies that focus on the condensation of highly detailed or near–explicit chemical mechanisms. For example, Jenkin et al. (2008) describe the development of a condensed Common Representative Intermediates (CRI) mechanism based on the explicit Master Chemical Mechanism (MCM v3.1), while Watson et al. (2008) describe the further reduction of the CRI mechanism and Utembe et al. (2009) describe the addition of SOA chemistry to the reduced mechanism. In our study, we have extended an existing condensed mechanism (CB05) that is an upgraded version of a mechanism (CB–IV) used routinely in urban and regional photochemical modeling for nearly two decades before being superseded by CB05. Emmerson and Evans (2009) compared several tropospheric gas–phase chemistry schemes, including CB–IV, for use within global models. CB05 itself has been tested during its development against smog chamber data (Yarwood et al., 2005), within a regional air quality model (Sarwar et al., 2008), and in an intercomparison of chemical mechanisms (Chen et al., 2010) based on data from the 2006 TexAQS II Radical and Aerosol Measurement Project (TRAMP–2006). Thus, the base mechanism for CB05_GE has been well tested, and the comparisons between CB05_GE and CB05 (with chlorine extensions) presented here can be considered as a "sanity check" to demonstrate that the global extensions to the mechanism do not have a significant effect on urban and regional photochemistry.

A zero–dimensional box model with a Rosenbrock solver was used for 24–hour simulations with the CB05Cl and CB05_GE mechanisms for conditions representative of both rural and urban regions. The simulations were conducted as purely initial value problems with no mixing, emissions, or removal by dry deposition. Note that the CB05Cl mechanism does not include either heterogeneous chemistry or bromine chemistry. Thus, for the CB05_GE case only, we conducted simulations with and without heterogeneous chemistry, and with and without initial bromine species concentrations. However, both mechanisms include chlorine chemistry, although the CB05_GE chlorine chemistry is more detailed, so simulations with and without initial chlorine species concentrations were also conducted for both mechanisms. For the mid–latitude tropospheric conditions used in these simulations, the CB05_GE results with zero initial bromine concentrations show very little difference from the full CB05_GE results, so that most of the differences between CB05Cl and CB05_GE can be attributed to differences in the heterogeneous chemistry and chlorine chemistry.

Figure 1 shows the variation of NO, NO_2 and O_3 concentrations over the 24–hour simulation period for the polluted urban case for the three mechanism configurations: CB05Cl, CB05_GE without heterogeneous chemistry, and CB05_GE. For all cases, the initial NO and O_3 in the system rapidly decrease due to their reaction forming NO_2. This phase is followed by the photochemical production of ozone with a peak ozone value of about 250 ppb 14 hours into the simulation (compared to the 100 ppb initial value). The results for CB05_GE without heterogeneous chemistry are virtually identical to the results with CB05Cl. However, when heterogeneous chemistry is included in the CB05_GE simulation, there are some differences between CB05Cl and CB05_GE, with slightly lower O_3 concentrations and slightly higher NO_2 concentrations predicted by CB05_GE. The peak O_3 concentration with CB05_GE with heterogeneous chemistry is about 8 ppb lower than the CB05Cl value or the CB05_GE value without heterogeneous chemistry.

The results for the clean rural case, shown in Figure 2, are qualitatively similar to the polluted case results, but there are some important differences. As in the polluted case, the peak ozone concentration predicted with the heterogeneous chemistry version of CB05_GE is about 8 ppb lower than the CB05Cl value. However, even when heterogeneous chemistry is turned off in CB05_GE, the predicted peak ozone concentration is slightly lower (about 2 ppb) than the CB05Cl value, suggesting that the differences in the chlorine chemistry mechanism between CB05Cl and CB05_GE become more important under clean conditions. When initial chlorine species concentrations are set to zero for the CB05Cl and CB05_GE (without heterogeneous chemistry and without bromine chemistry), the results from the two mechanisms are identical.

3.2. Testing of extensions to base mechanism

The same box model used in Section 3.1 was used to conduct 24–hour simulations to evaluate the extensions to the base CB05Cl mechanism for three representative scenarios: upper troposphere, lower stratosphere, and marine Arctic scenario. The first two scenarios are conducted for a summer day (July) at different heights (10 km for upper troposphere, and 20 km for lower stratosphere). The last scenario (Arctic) corresponds to a spring day in late March at 82^{o}N and 62^{o}W, Nunavut in Canada, and is conducted to simulate O_3 and Hg Arctic depletion events (e.g.,

Bottenheim et al., 2002a; Spicer et al., 2002; Steffen et al., 2002; Skov et al., 2004). Initial mixing ratios for many species for the upper troposphere and lower stratosphere simulations are based on boundary conditions for the western U.S. from a global model (GEOS–CHEM) provided by Harvard University for a previous regional modeling application (Karamchandani et al., 2010), and on observed values for the Arctic scenario simulations. Note that other global CTMs with more detailed treatment of stratospheric chemistry and dynamics than GEOS–Chem may possibly provide a more realistic representation of stratospheric concentrations, and using GEOS–CHEM for the initialization of the upper troposphere and lower stratosphere box model simulations described here may introduce some uncertainties in our results. However, the GEOS–Chem results were easily accessible and adequate for the qualitative testing described here. A more detailed evaluation of the mechanism will be conducted within the GU–WRF/Chem framework that will include a detailed treatment of stratospheric chemistry and dynamics.

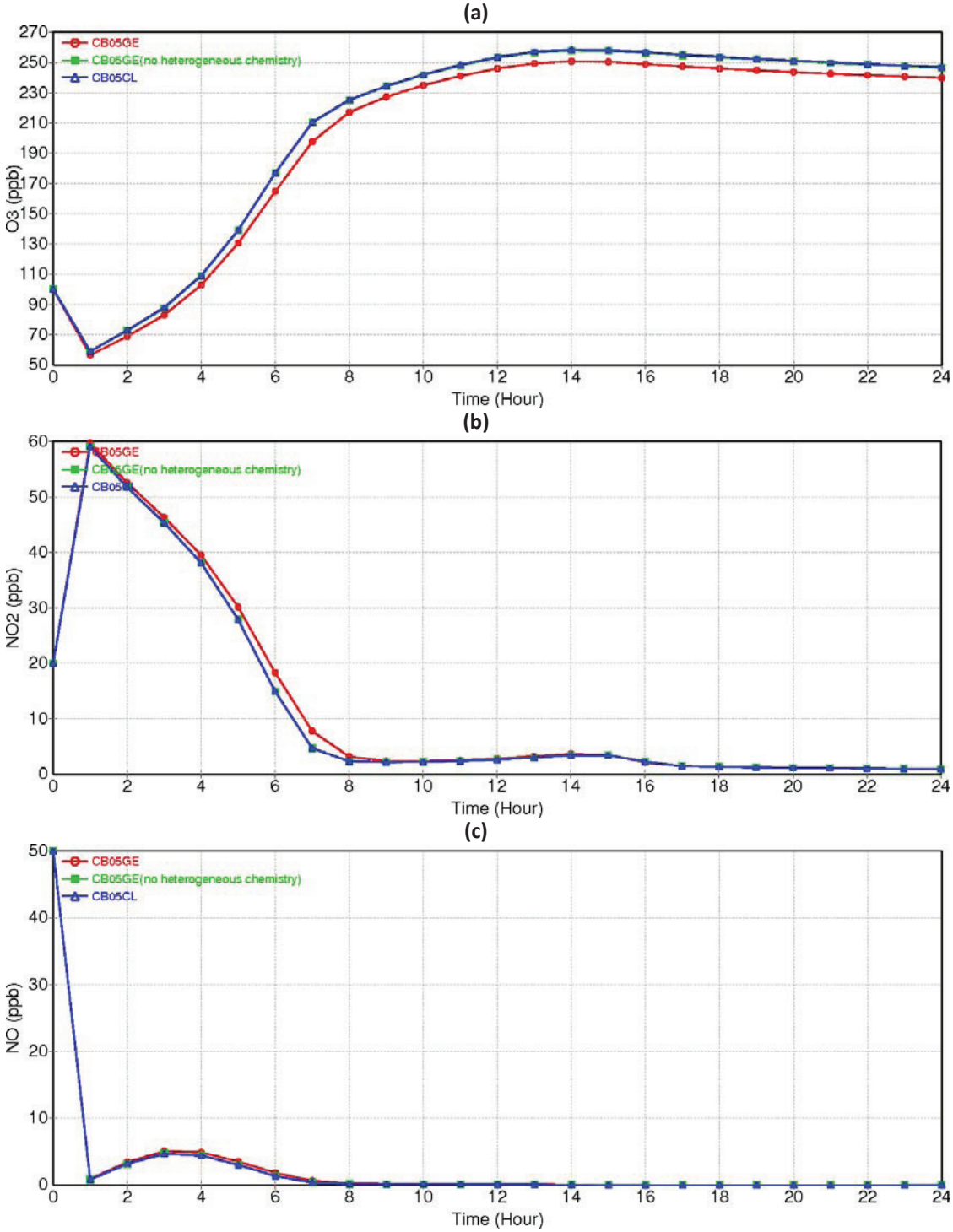

Figure 1. *Diurnal variations in (a) NO, (b) NO_2 and (c) O_3 mixing ratios for polluted (urban) tropospheric simulations with the base mechanism (CB05Cl), the extended mechanism (CB05GE), and the extended mechanism without heterogeneous chemistry.*

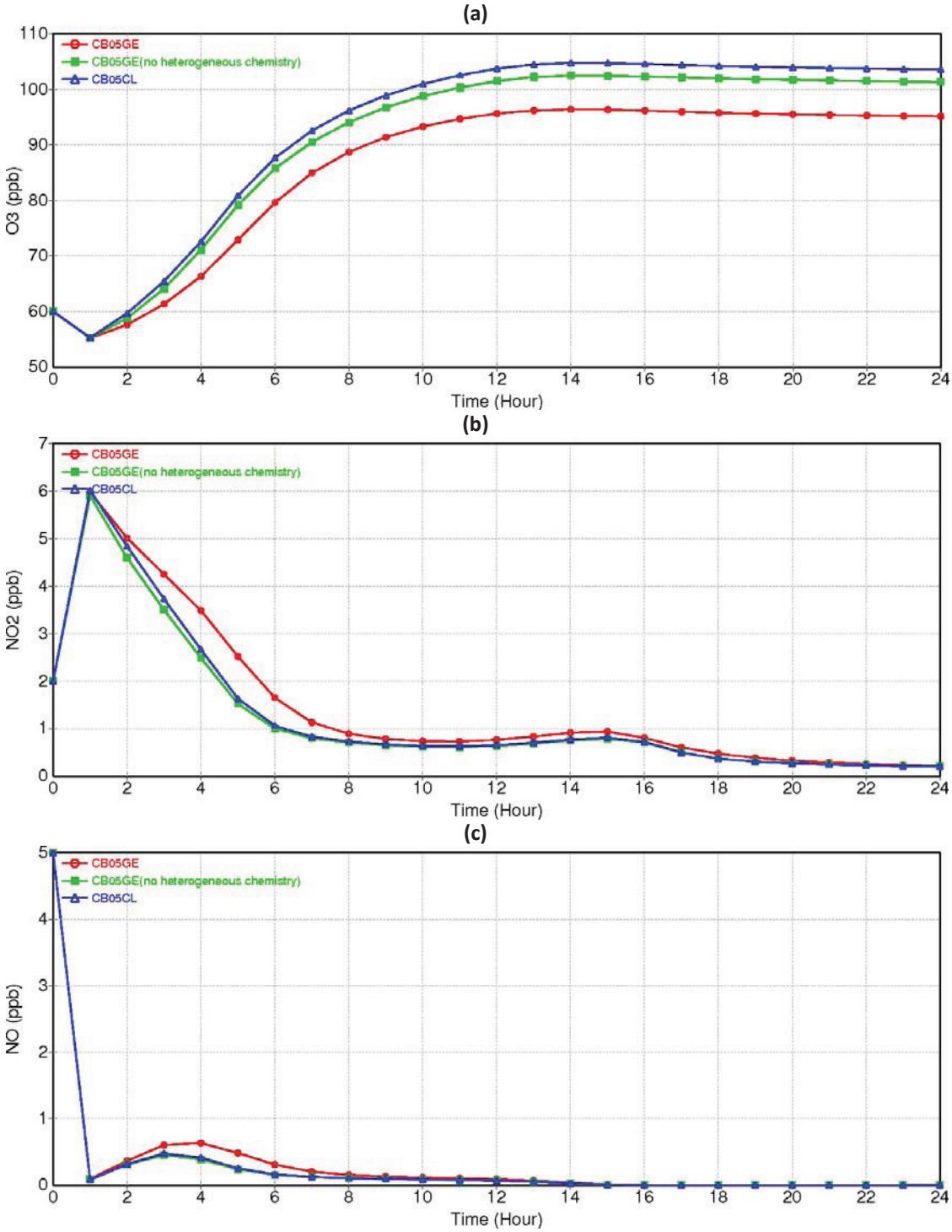

Figure 2. *Diurnal variations in (a) NO, (b) NO_2 and (c) O_3 mixing ratios for clean (rural or regional) tropospheric simulations with the base mechanism (CB05Cl), the extended mechanism (CB05GE), and the extended mechanism without heterogeneous chemistry.*

Three simulations are conducted for each scenario: without chlorine and bromine species (NoClBr); with chlorine but no bromine species (NoBr); and with chlorine and bromine species (ClBr). Simulations with and without heterogeneous chemistry are also conducted for the upper troposphere, lower stratosphere, and Arctic scenarios to study their role in O_3 and Hg depletion for these scenarios. For the simulations with halogen species, an initial total inorganic chlorine mixing ratio of 1 ppb and initial total inorganic bromine mixing ratio of 34 ppt are assumed as upper bounds. Typical chlorine mixing ratios in the marine boundary layer are of the order of 0.5 ppb (e.g., Chang et al., 2004; Finlayson–Pitts, 2010). Bromine mixing ratios of the order of 30 ppt and higher have been measured in the Arctic (e.g., Tuckermann et al., 1997; Martinez et al., 1999; Foster et al., 2001; Honninger and Platt, 2002, Spicer et al., 2002, Finlayson–Pitts, 2010). The initial mixing ratios of mercury species are specified as 0.2 ppt for elemental mercury and 0.002 ppt for divalent mercury. These values are typical of measured background concentrations of these species (e.g., Ebinghaus et al., 2002; Calvert and Lindberg, 2003; Seigneur et al., 2006; Fain et al., 2009). Mixing ratios of molecular oxygen, methane and hydrogen are specified as 210 000 ppm (21% of air), 1.85 ppm and 0.56 ppm, respectively. The initial concentrations of all other species vary according to the different scenarios as described below and shown in Table 6.

Table 6. *Initial conditions for the box model simulations*

Species	Mixing Ratios[a]		
	Arctic Scenario	Upper Troposphere Scenario	Lower Stratosphere Scenario
NO	15 ppt		
NO_2	30 ppt	20 ppt	500 ppt
HONO	50 ppt	50 ppt	5 ppt
HNO_3	200 ppt	100 ppt	3 ppb
O_3	40 ppb	35 ppb	800 ppb
N_2O			300 ppb
H_2O_2	200 ppt	200 ppt	
CO	180 ppb	56 ppb	20 ppb
FORM	200 ppt	60 ppt	
ALD2	170 ppt		
ALDX	30 ppt		
PAN	50 ppt	30 ppt	1 ppt
PAR	1 ppb	7 ppb	
OLE	500 ppt		
IOLE	500 ppt		
ETH	500 ppt		
TOL			
XYL			
Cl_2	1 ppb	1 ppb	1 ppb
CH_3Cl	500 ppt	500 ppt	500 ppt
$CFCl_3$		300 ppt	300 ppt
CF_2Cl_2		500 ppt	500 ppt
Br	4 ppt	4 ppt	4 ppt
BrO	30 ppt	30 ppt	30 ppt
CH_3Br	10 ppt	10 ppt	10 ppt
CF_2ClBr		1.7 ppt	1.7 ppt
CF_3Br		2 ppt	2 ppt
Hg(0)	0.2 ppt	0.2 ppt	0.2 ppt
Hg(2)	0.002 ppt	0.002 ppt	0.002 ppt

[a] *Based on available observed values (Arctic scenario) or GEOS-CHEM values (upper troposphere and lower stratosphere scenarios) for most species.*

The box model results for the Arctic, upper troposphere and lower stratosphere scenarios are presented below. As mentioned previously, the box model also includes aerosol and aqueous–phase chemistry modules. However, our focus in this paper is the CB05_GE mechanism and the box model results are analyzed in terms of the effect of extensions to CB05, including halogen and heterogeneous chemistry, on O_3 and mercury concentrations. For the simulations with heterogeneous chemistry, we specify surface areas and background values of total particulate matter (PM) concentrations, instead of explicitly calculating the concentrations of PM components within the box model.

Marine ARCTIC scenario. Typical initial mixing ratios (see Table 6) of NO_x ($NO + NO_2$), NO_z (NO_x oxidation products), O_3, H_2O_2, and volatile organic compounds (VOCs) such as alkenes, formaldehyde and acetaldehyde are specified under the Arctic scenario based on Arctic field study measurements (e.g., Li, 1994; Bottenheim et al., 2002a, 2002b; Sumner et al., 2002; Boudries et al., 2002). The simulations are performed both with and without heterogeneous chemistry on Arctic aerosols.

Figure 3a shows the temporal variations of O_3 mixing ratios for the NoClBr, NoBr and ClBr simulations without heterogeneous chemistry. For the case without halogens, a slight (0.3%) depletion in O_3 mixing ratios occurs at the end of the simulation. When chlorine is added, nearly 5% of the initial O_3 is depleted at the end of 24 hours. When bromine is also added, more than 5% of the initial O_3 is depleted at the end of 24 hours. As shown in Figure 3b, adding bromine results in some depletion of Hg(0). More than 2% of the initial Hg(0) is depleted at the end of 24 hours in the ClBr simulation compared to less than 0.5% in the case with no halogen chemistry. Correspondingly, Figure 3c shows that the divalent mercury at the end of 24 hours in the ClBr simulation is more than twice the divalent mercury in the NoClBr simulation.

These results show much lower O_3 and Hg depletion than has been observed during Arctic depletion events (e.g., Schroeder et al., 1998; Foster et al., 2001; Bottenheim et al., 2002a; Lindberg et al., 2002; Spicer et al., 2002; Skov et al., 2004). An analysis of the box–model simulation results shows that the lower depletion in the simulation occurs because most of the initial specified reactive bromine (Br and BrO) and chlorine are converted to stable products (mainly HBr and small amounts of HOBr and $BrONO_2$ in the case of bromine and HCl, formyl chloride, HOCl and $ClONO_2$ in the case of chlorine). As noted by von Glasow et al. (2004), the cycling of HOBr, HBr and $BrONO_2$ is very slow when only gas–phase reactions are included, and it is necessary to include heterogeneous reactions on aerosol particles and sea–ice surfaces to cycle the reactive bromine and chlorine. The importance of heterogeneous reactions for Arctic boundary layer chemistry and sustained ozone depletion has also been noted in several other studies (e.g., Fan and Jacob, 1992; Abbat, 1994; Abbat and Nowak, 1996; Lary et al., 1996; Huff and Abbat, 2000; Jacob, 2000; Lehrer et al., 2004).

Figure 4 shows the results for the Arctic scenario simulations when heterogeneous chemistry is activated. As shown in Figure 4a, for the case without halogens (NoClBr), there is a slight (0.3%) depletion in O_3 mixing ratios at the end of the simulation comparable to the depletion in the simulation without heterogeneous chemistry. When chlorine is added, more than 5% of the initial O_3 is depleted at the end of 24 hours. When bromine is also added, nearly 7% of the initial O_3 is depleted at the end of 24 hours. Figures 4b and 4c show that adding bromine results in a depletion of Hg(0) of nearly 5% in 24 hours (about twice the amount depleted in the simulation without heterogeneous chemistry).

Adding heterogeneous chemistry thus has a noticeable effect on the O_3 and Hg depletion. The differences between the simulations with and without heterogeneous chemistry are highlighted in Figure 5. However, even with heterogeneous chemistry, the simulated depletion is significantly lower than that observed during some springtime depletion events. A detailed examination of the results indicates that both HCl and HBr are formed efficiently by the reactions of chlorine and bromine atoms with formaldehyde and acetaldehyde. The role of formaldehyde as a sink for Br atoms has been noted in previous studies (e.g., Sumner et al., 2002; Grannas et al., 2002). In our box model simulations, formaldehyde and other carbonyl compounds are present either from the initial conditions specification, or formed by the reactions of chlorine atoms with hydrocarbons such as alkanes and alkenes. Thus, even though the heterogeneous chemistry liberates reactive chlorine and bromine from the stable reservoir species, the reactive species form the stable products rapidly by reacting with the primary and secondary formaldehyde.

Interestingly, it should also be noted that Calvert and Lindberg (2003) used a gas–phase only mechanism and simulated higher O_3 and Hg depletion rates than those simulated here. The key differences between their study and our study is that their mechanism did not include the reactions between Br and acetaldehyde and Br and the HO_2 radical (Reactions 57 and 64, respectively in Table 2) to form the stable HBr product. Furthermore, their initial bromine concentrations were factors of 4 to 10 higher than those used in this study. When Reactions 57 and 64 in Table 2 are deactivated and higher initial reactive bromine concentrations are used in our box model simulations, the simulated depletion rates become comparable to those obtained by Calvert and Lindberg (2003).

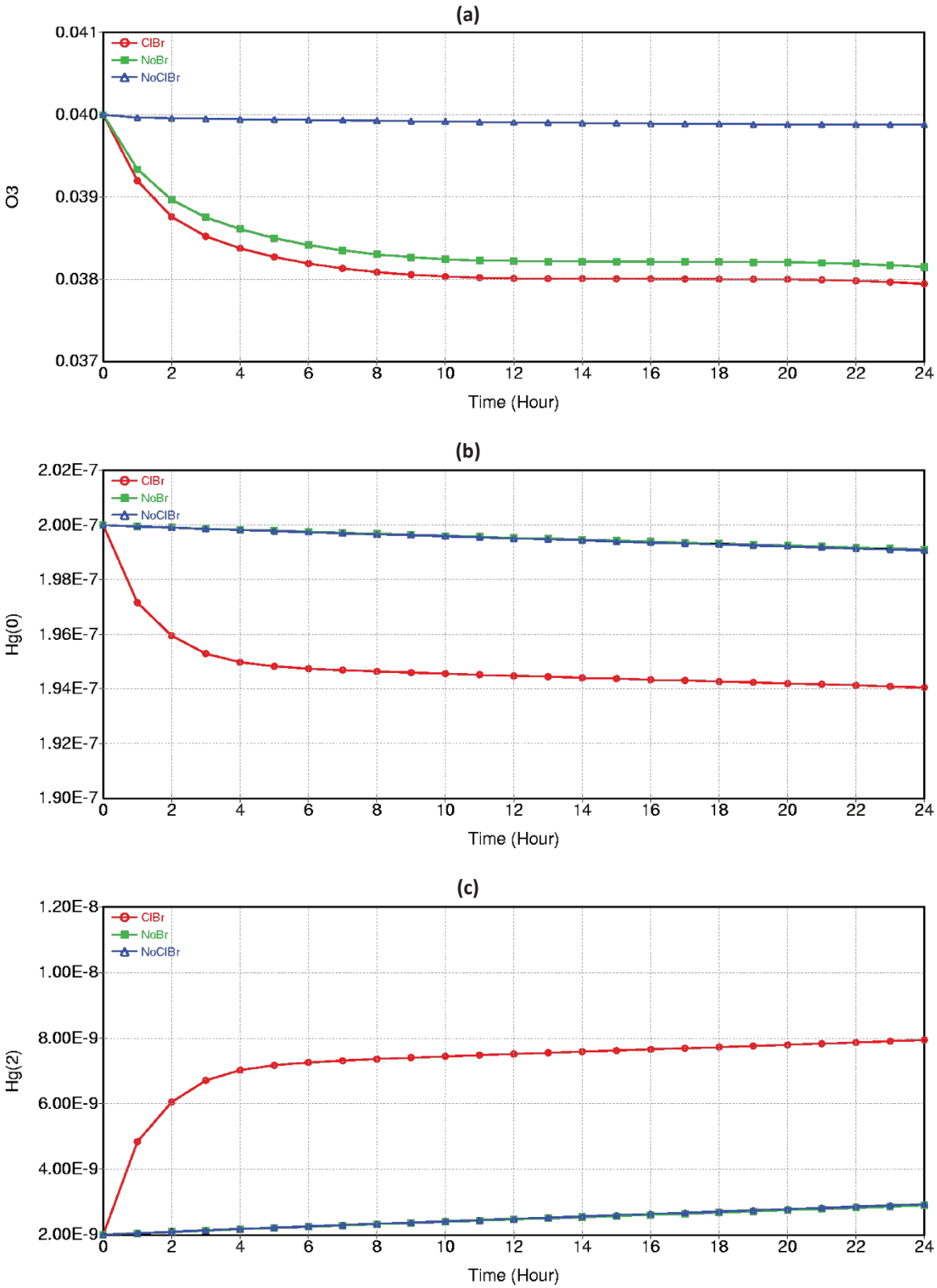

Figure 3. *Diurnal variations in (a) O_3, (b) Hg(0) and (c) Hg(2) mixing ratios for a marine Arctic scenario simulation without heterogeneous chemistry. The blue line (NoClBr) represents the case with no halogen chemistry, the green line represents the case with chlorine chemistry, and the red line represents the case with chlorine and bromine chemistry.*

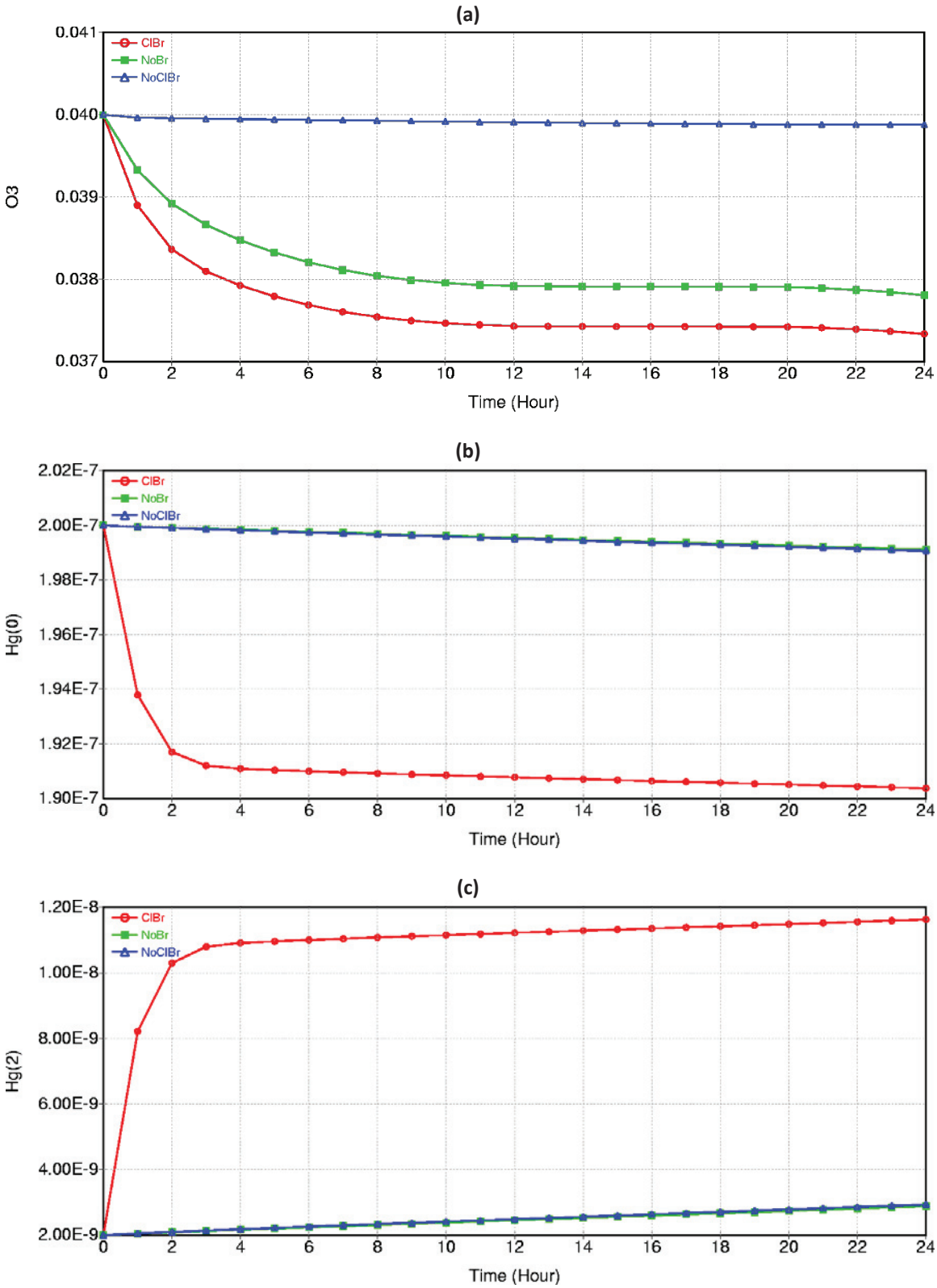

Figure 4. *Diurnal variations in (a) O_3, (b) Hg(0) and (c) Hg(2) mixing ratios for a marine Arctic scenario simulation with heterogeneous chemistry. The blue line (NoClBr) represents the case with no halogen chemistry, the green line represents the case with chlorine chemistry, and the red line represents the case with chlorine and bromine chemistry.*

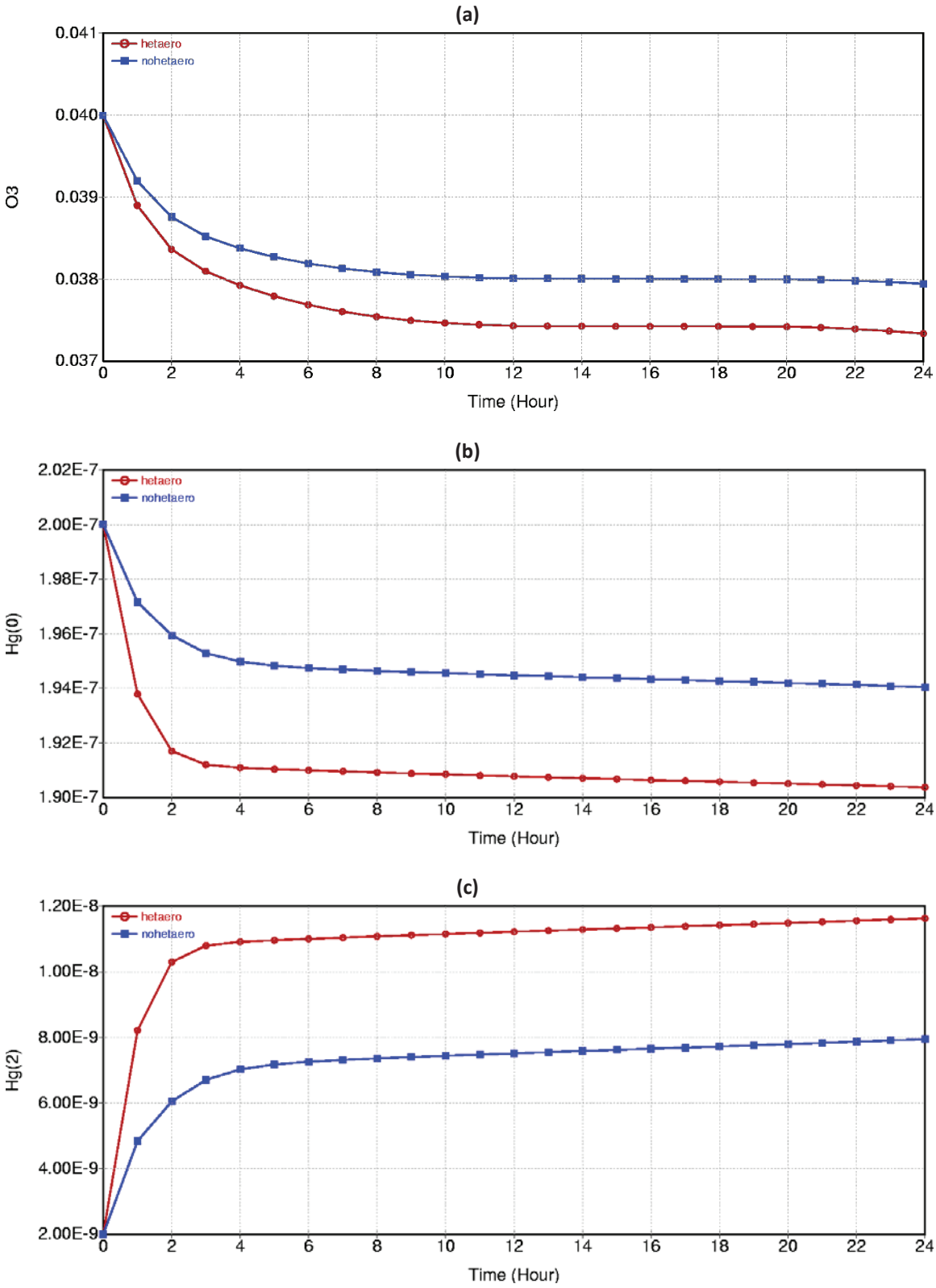

Figure 5. *Diurnal variations in (a) O_3, (b) Hg(0) and (c) Hg(2) mixing ratios for a marine Arctic scenario simulation with chlorine and bromine chemistry. The blue line represents the case with no heterogeneous chemistry, while the red line represents the case with heterogeneous chemistry.*

The observed extreme O_3 and Hg(0) depletion events in the Arctic could be therefore due to a combination of conditions such as extremely low VOC and aldehyde concentrations, cold temperatures, and availability of bromine and chlorine sources. Ariya et al. (1999) and Eneroth et al. (2007) and references cited therein have noted decreases in hydrocarbon concentrations during ozone depletion episodes. Hydrocarbon measurements made during the ARCTOC 95 and ARCTOC 96 field campaigns also show that alkane and ethyne mixing ratios decrease during ozone depletion events (Ramacher, et al., 1997; Ramacher, et al., 1999). However, these decreases are likely due to reactions of the organic compounds with chlorine atoms and not necessarily to low VOC concentrations prior to the depletion episodes (e.g., Ramacher et al., 1999). As suggested by Friess et al. (2004), Hopper et al. (1998) and Morin et al. (2005), it is likely that the intense ozone depletion episodes occur as a result of stable air mass conditions and the

presence of active halogen emission sources that provide a steady supply of chlorine and bromine during these episodes. While these processes can be simulated in dynamical box models or in the WRF/Chem model where the CB05_GE mechanism is implemented, the box model used in this study is limited in its capabilities to simulate this behavior. However, it is still informative to use the box model in its current form to understand the influence of reactive halogen stabilizing species, such as formaldehyde, on the ozone depletion process. We do this by conducting additional simulations with zero initial concentrations of VOCs and aldehydes, with and without heterogeneous chemistry, for the Arctic scenario. This approach indirectly simulates conditions during intense depletion episodes by eliminating a removal term for active halogen species.

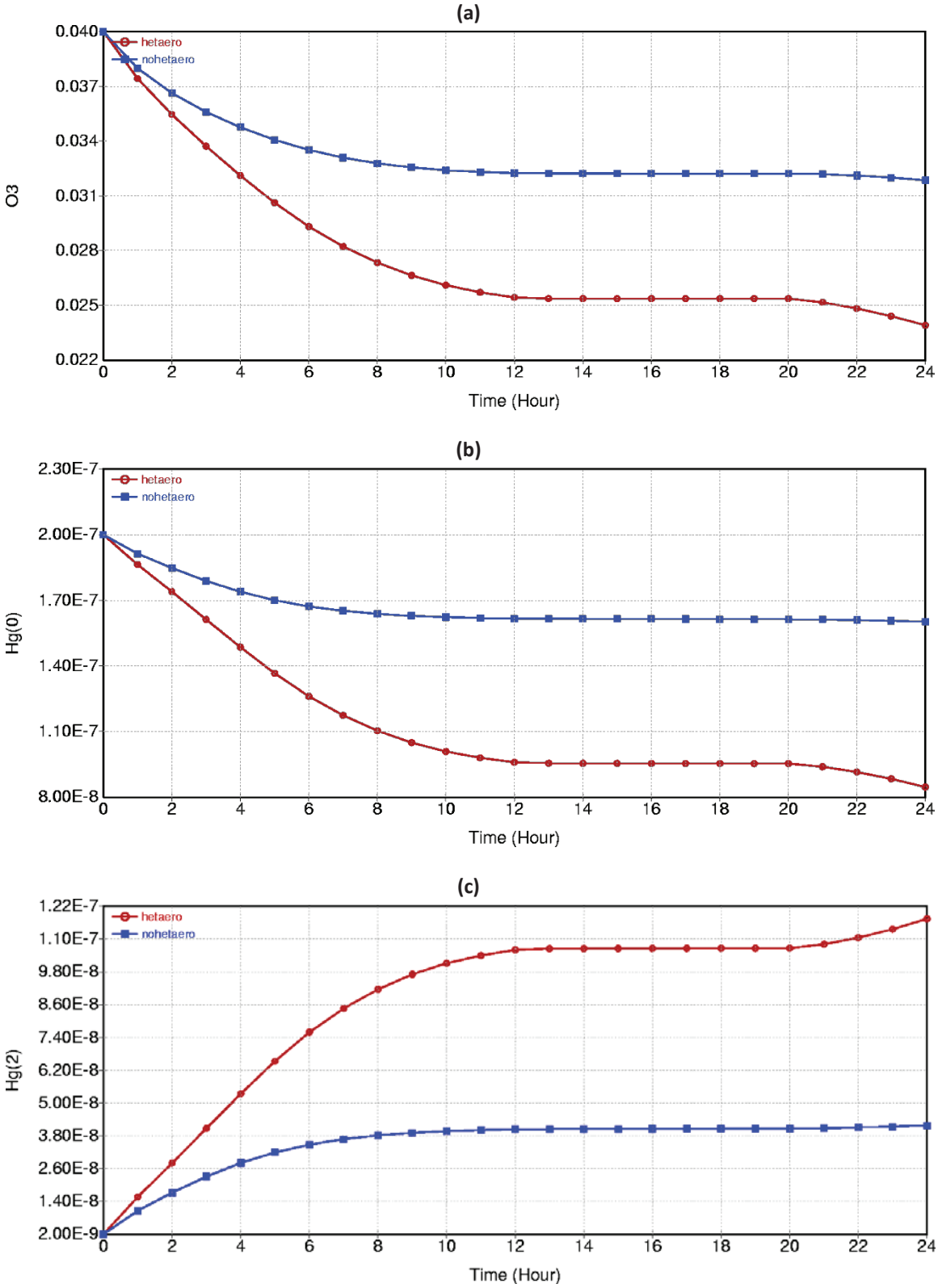

Figure 6. *Diurnal variations in (a) O_3, (b) Hg(0) and (c) Hg(2) mixing ratios for a marine Arctic scenario simulation with chlorine and bromine chemistry and zero initial hydrocarbons and aldehydes. The blue line represents the case with no heterogeneous chemistry, while the red line represents the case with heterogeneous chemistry.*

Figure 6 illustrates the differences between the simulations with and without heterogeneous chemistry for conditions with zero initial VOC and aldehyde concentrations. As shown in Figure 6a, over 20% of the initial O_3 is depleted without heterogeneous chemistry. The depletion for the heterogeneous chemistry case is over 40%, about a factor of two more than the depletion in the non–heterogeneous chemistry case. Figure 6b shows that, in the case of Hg(0), the heterogeneous chemistry results in nearly 58% depletion. This depletion is nearly 3 times the 20% depletion in the simulation without heterogeneous chemistry. These depletion extents are much more comparable to some of the extreme depletion events observed in the Arctic where O_3 levels drop by 20 ppb or more (e.g., Simpson et al., 2007).

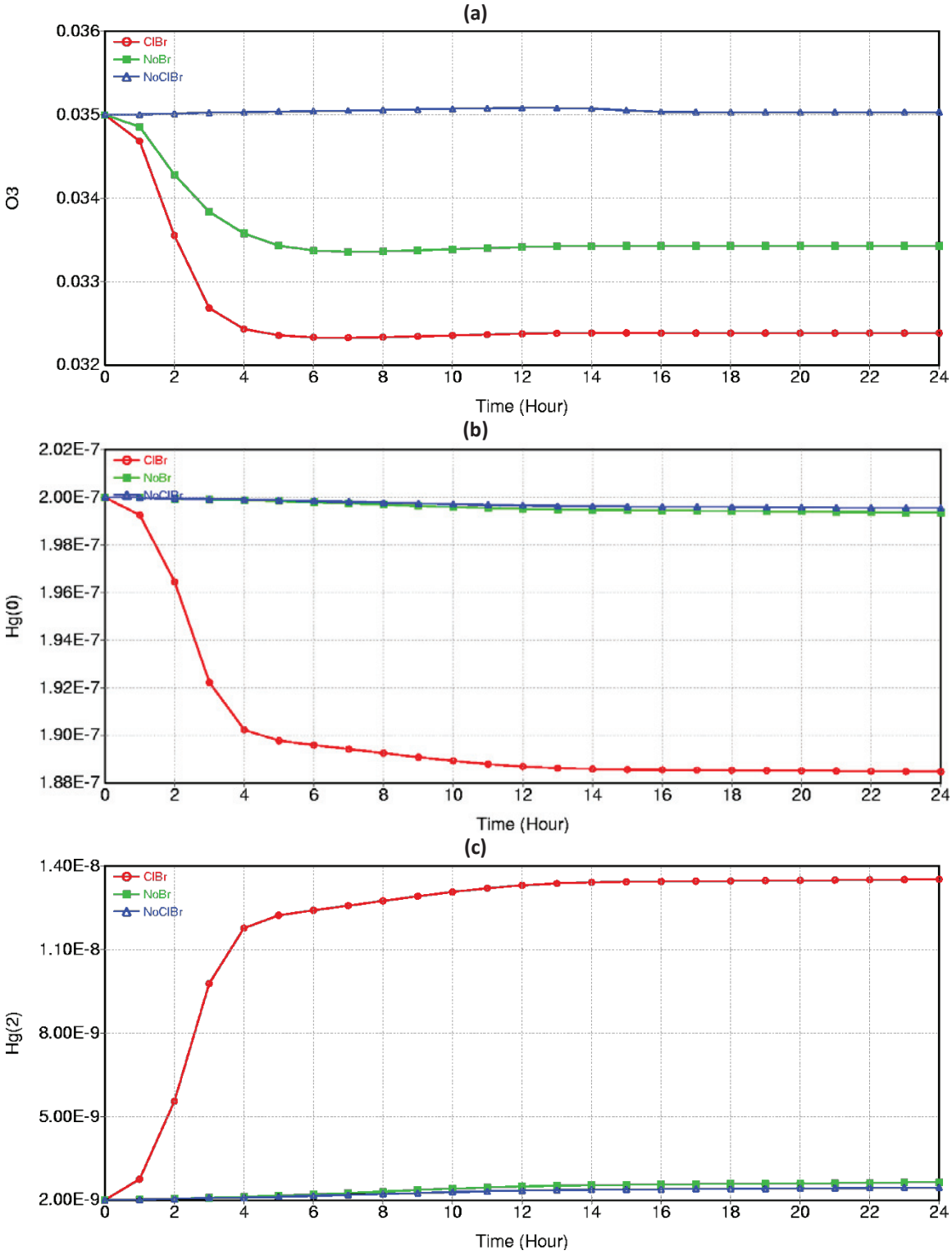

Figure 7. *Diurnal variations in (a) O_3, (b) Hg(0) and (c) Hg(2) mixing ratios for an upper troposphere scenario simulation. The blue line (NoClBr) represents the case with no halogen chemistry, the green line represents the case with chlorine chemistry, and the red line represents the case with chlorine and bromine chemistry.*

Upper troposphere scenario. Typical initial mixing ratios of NO_x, NO_z, O_3, H_2O_2 and VOCs (see Table 6) are specified for the upper tropospheric scenario based on GEOS–CHEM outputs provided by Harvard University for a previous continental U.S. modeling study (Karamchandani et al., 2010). The temporal variations of O_3 mixing ratios for the NoClBr, NoBr and ClBr simulations are shown in Figure 7a. For the case without halogen chemistry, some small photochemical production of O_3 occurs. For both the NoBr case (i.e., chlorine chemistry only) and the full halogen chemistry case, the O_3 mixing ratio is depleted during the first 7 to 8 hours followed by a small recovery. As expected, the O_3 depletion is higher when both chlorine and bromine are included as compared to the case with chlorine only. The maximum O_3 depletion for the former case is nearly 7.5%, while the maximum depletion for the latter case is about 4.5%. As shown in Figure 7b, there is an increase in Hg(0) depletion when bromine is included, with nearly 6% of the initial Hg(0) depleted at the end of 24 hours. Figure 7c shows that the Hg(2) concentration at the end of 24 hours in the ClBr simulation is nearly six times that in the NoClBr simulation.

The results shown in Figure 7 are for the case when heterogeneous chemistry is simulated. Without heterogeneous chemistry (not shown here), the Hg(0) depletion is about 3%, nearly a factor of two lower than the depletion with heterogeneous chemistry.

Lower stratosphere scenario. As in the upper troposphere scenario, available outputs from GEOS–CHEM are used to specify typical initial mixing ratios of NO_x, NO_z, O_3, H_2O_2 and VOCs for the lower stratosphere scenario. The initial O_3 mixing ratio is 800 ppb under this scenario, which is about 20 times larger than the upper troposphere value of 35 ppb and the Arctic scenario value of 40 ppb. However, the air density at 20 km altitude is about 15 times lower than the air density at the surface and about 4 times lower than the air density at 10 km in the upper troposphere scenario. Thus, on a mass basis there is less difference between the O_3 concentrations in the lower stratosphere scenario and the other scenarios than on a mixing ratio basis. However, the chlorine and bromine mixing ratios for the lower stratosphere scenario are the same as in all the other scenarios, so the relative difference between O_3 concentrations and halogen concentrations is much higher in the lower stratosphere scenario. To understand the effect of these differences between the upper troposphere and lower stratosphere scenarios, we also conducted a simulation with bromine but no chlorine (NoCl) for the lower stratosphere scenario.

Three sets of simulations were conducted for the lower stratosphere scenario. In the first set, heterogeneous reactions on Type I PSCs were included. In the second set, heterogeneous reactions on Type II PSCs are included. In the third set, heterogeneous reactions on all PSCs are deactivated. Figure 8 shows the results from the first set of simulations. As shown in Figure 8a, when only bromine is included (NoCl), there is a slight (0.7%) increase in the O_3 depletion. On the other hand, when only chlorine is included (NoBr), the amount of O_3 depleted at the end of 24 hours is about 35 ppb (4.3%), nearly 30 ppb more than is depleted in the NoCl case. Finally, when both chlorine and bromine are included, 65 ppb of the initial O_3 is depleted at the end of 24 hours. This depletion of O_3 is over 8%, comparable to the depletion in the upper troposphere simulation.

The corresponding results for Hg(0) and Hg(2) are shown in Figures 8b and 8c, respectively. As compared to the Arctic and upper troposphere scenarios, Hg(0) depletion rates are actually lower in the NoBr and ClBr simulations than in the simulation with no halogens. The largest depletion is for the NoCl (bromine only) simulation. It appears from these results that the other Hg(0) oxidation pathways (reactions with O_3 and OH) also play an important role in the lower stratosphere scenario. This can be attributed to both the higher O_3 (and OH) to halogen ratios in this scenario compared to the Arctic and upper troposphere scenarios, as well as the fact that the bromine oxidation rate is directly proportional to the atmospheric pressure, which is very low at 20 km. When only chlorine is included (NoBr), the resulting depletion in O_3 reduces the Hg(0) oxidation from these other pathways. When bromine is also included (ClBr), there is additional O_3 depletion (Figure 8a) resulting in even lower Hg(0) oxidation from the other pathways, but this is somewhat compensated by the bromine oxidation reactions. Finally, when only bromine is included (NoCl), the O_3 depletion is lower (as shown in Figure 8a) and the bromine oxidation pathway is also active, resulting in higher oxidation of Hg(0) to Hg(2).

The results when heterogeneous reactions on Type II PSCs are included are qualitatively similar to those for Type I PSCs, as shown in Figure 9. However, Type II PSCs are expected to be more efficient than Type I PSCs at liberating reactive chlorine and bromine from the stable forms of these species, based on the reaction probabilities shown in Table 5 (e.g., Jacobson, 2005). Thus, higher O_3 and mercury depletions on Type II PSCs are expected as compared to the depletions with Type I PSCs. This is indeed the case as shown in Figures 8 and 9. Figure 9a shows that, when only bromine is included (NoCl), there is a slight increase in the O_3 depletion as in the Type I PSC simulation. When only chlorine is included (NoBr), the amount of O_3 depleted at the end of 24 hours is about 48 ppb (6%), about 13 ppb more than the depletion in the corresponding Type I PSC simulation. Finally, when both chlorine and bromine are included, 87 ppb or nearly 11% of the initial O_3 is depleted at the end of 24 hours, about 22 ppb more than the depletion in the corresponding Type I PSC simulation.

In the case of Hg(0) depletion, as shown in Figure 9b, without chlorine and bromine chemistry (NoClBr), nearly 9% of the Hg(0) is depleted in the presence of Type II PSCs, comparable to the depletion with Type I PSCs, shown in Figure 8b. This is expected because the differences between the Type I PSC and Type II PSC simulations will be manifested primarily in the presence of halogens. When both chlorine and bromine species are present (ClBr), the depletion for the Type II PSC simulation is still about 9%, but is a little higher than the depletion for the Type I PSC simulation (about 8%). When only chlorine is present (NoBr), the Hg(0) depletion for the Type II PSC simulation drops to about 5.5%, compared to the depletion of about 5.1% for the Type I PSC simulation. As discussed previously, this drop is related to the depletion of the O_3 and consequently, OH, concentrations in the presence of chlorine, which results in a decrease in the oxidation rate of Hg(0) by OH and O_3. Finally, when only bromine is present (NoCl), the elemental mercury depletion in the Type II PSC simulation is about 11%, a little higher than that in the Type I PSC simulation (about 10%).

Figure 10 shows the effect of heterogeneous PSC chemistry in the presence of chlorine and bromine on O_3 and Hg(0) depletion and Hg(2) formation. As expected, the slowest depletion occurs when PSCs are not present, and the depletion rates for Type II PSCs are larger than those for Type I PSCs.

Half–life of Hg(0). The results presented above show that, for most conditions, oxidation by Br and BrO is generally the most important pathway for Hg(0) depletion. However, the lower stratospheric simulation with high initial O_3 mixing ratios (representative of the lower stratosphere) shows that oxidation by other pathways, in particular by OH, can become important under certain conditions. The roles of various Hg(0) oxidation pathways can be quantified by calculating the approximate Hg(0) half–lives for the different Hg(0) oxidation pathways (O_3, OH, H_2O_2 and Br/BrO) for the various scenarios. These half–life values are calculated by turning off all but one oxidation pathway and calculating an effective first–order rate constant for each pathway from the Hg(0) concentrations at

the beginning and end of the simulation. The half–lives are listed in Table 7. Table 7 shows that the O_3 and H_2O_2 oxidation pathways for Hg(0) are generally slow. Hg(0) half–lives for O_3 oxidation ranging from about 3 000 hours for the lower stratosphere scenario to about 24 000 hours for the upper troposphere scenario, while the half–lives for H_2O_2 oxidation range from about 18 000 hours for the Arctic scenario to more than 650 000 hours for the lower stratosphere scenario. The OH oxidation pathway is slow for the Arctic and upper troposphere scenarios, but is the fastest for the lower stratosphere scenarios (half–life of 345 hours for Type I PSCs and 330 hours for Type II PSCs). The bromine oxidation pathway is the fastest of all the pathways for the Arctic and upper troposphere scenarios. In particular, the bromine oxidation pathway is very efficient (half–life of less than one day) for the Arctic scenario simulation when initial VOC and aldehyde concentrations are set to zero to indirectly simulate conditions in which active sources of halogen atoms are available to replenish the atoms converted to stable species by their reactions with carbonyl compounds.

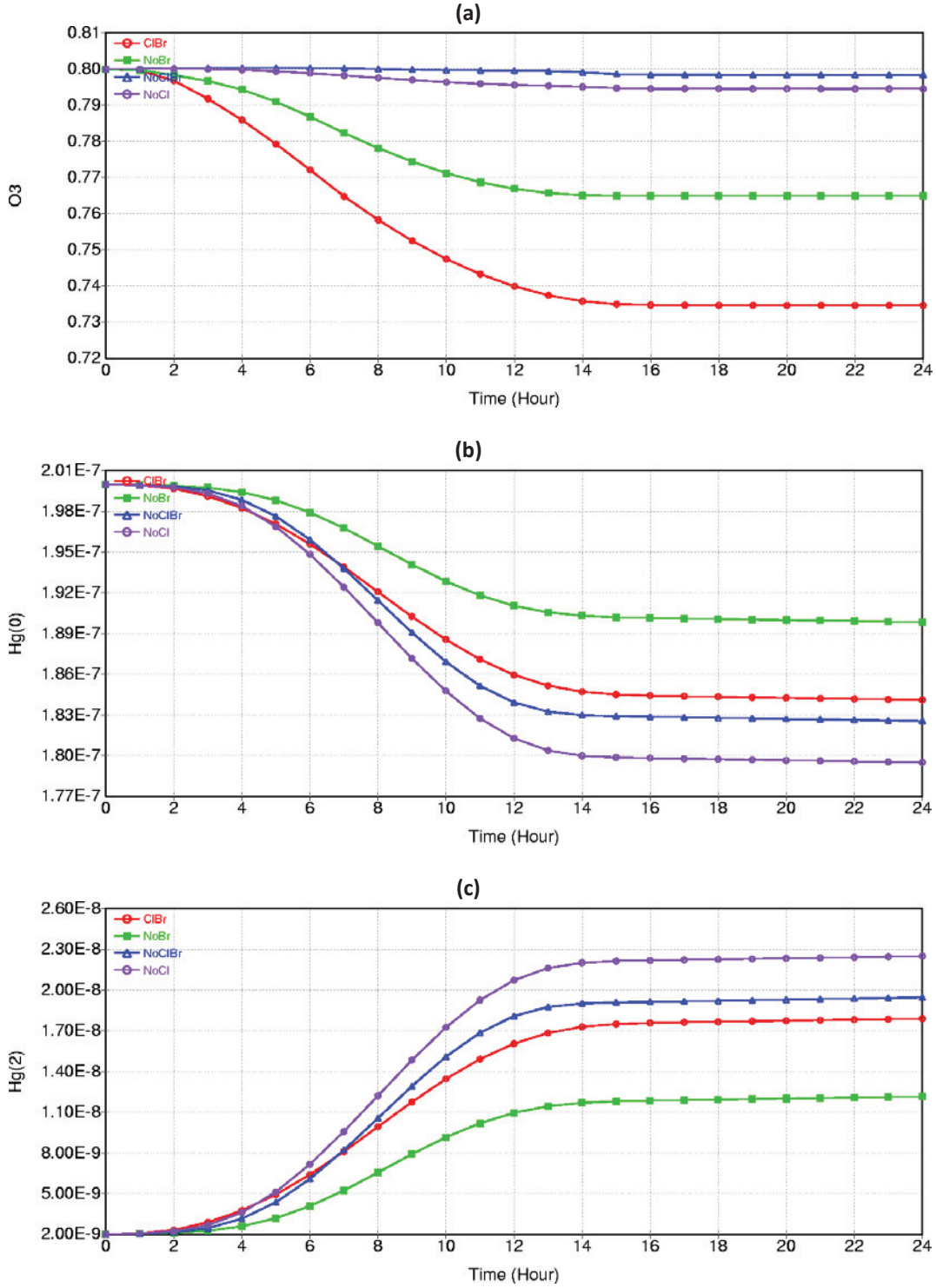

Figure 8. *Diurnal variations in (a) O_3, (b) Hg(0) and (c) Hg(2) mixing ratios for a lower stratosphere scenario simulation with heterogeneous reactions on Type I PSCs. The blue line (NoClBr) represents the case with no halogen chemistry, the green line represents the case with chlorine chemistry, the purple line represents the case with bromine chemistry and the red line represents the case with both chlorine and bromine chemistry.*

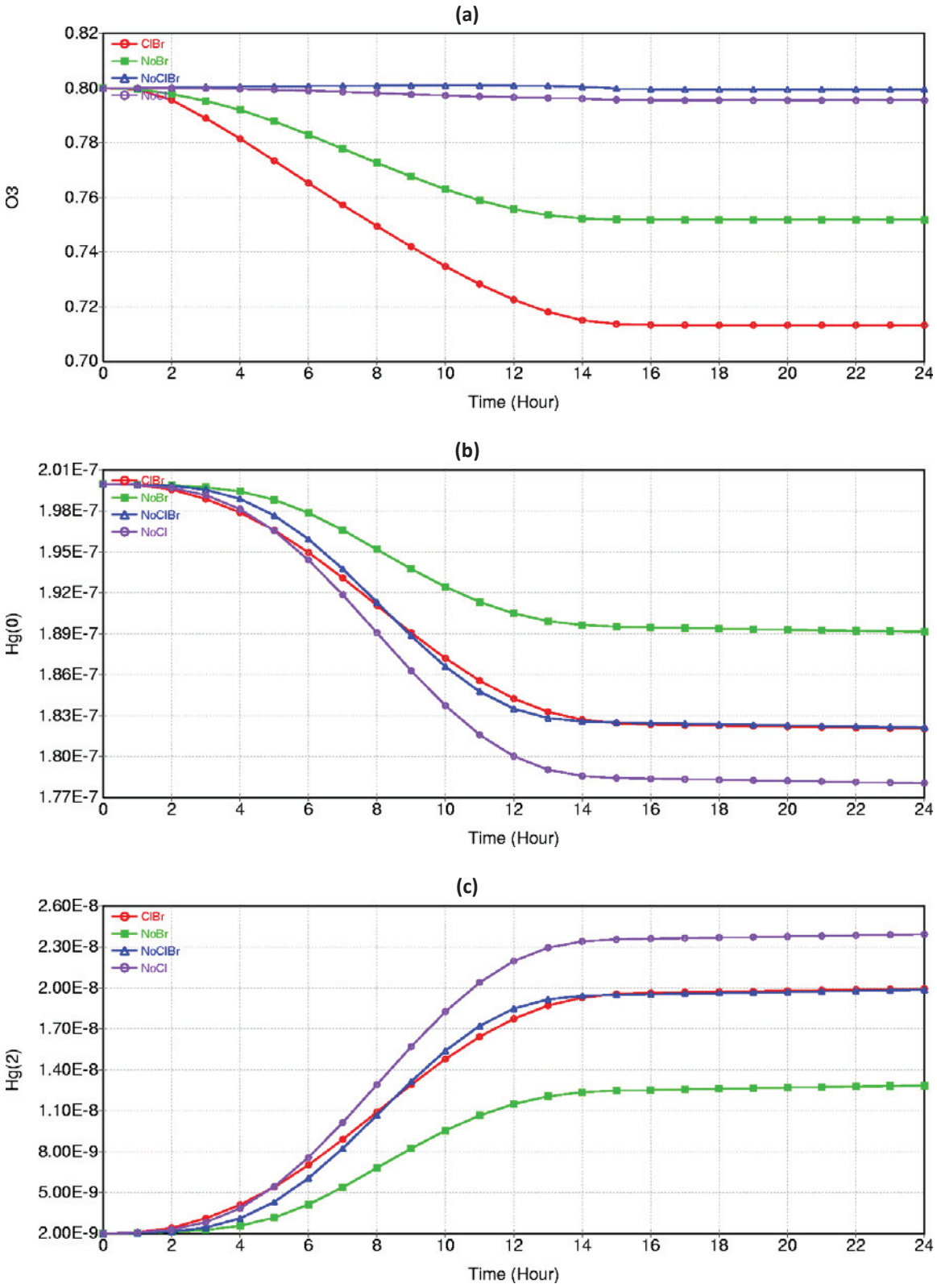

Figure 9. *Diurnal variations in (a) O_3, (b) Hg(0) and (c) Hg(2) mixing ratios for a lower stratosphere scenario simulation with heterogeneous reactions on Type II PSCs. The blue line (NoClBr) represents the case with no halogen chemistry, the green line represents the case with chlorine chemistry, the purple line represents the case with bromine chemistry and the red line represents the case with both chlorine and bromine chemistry.*

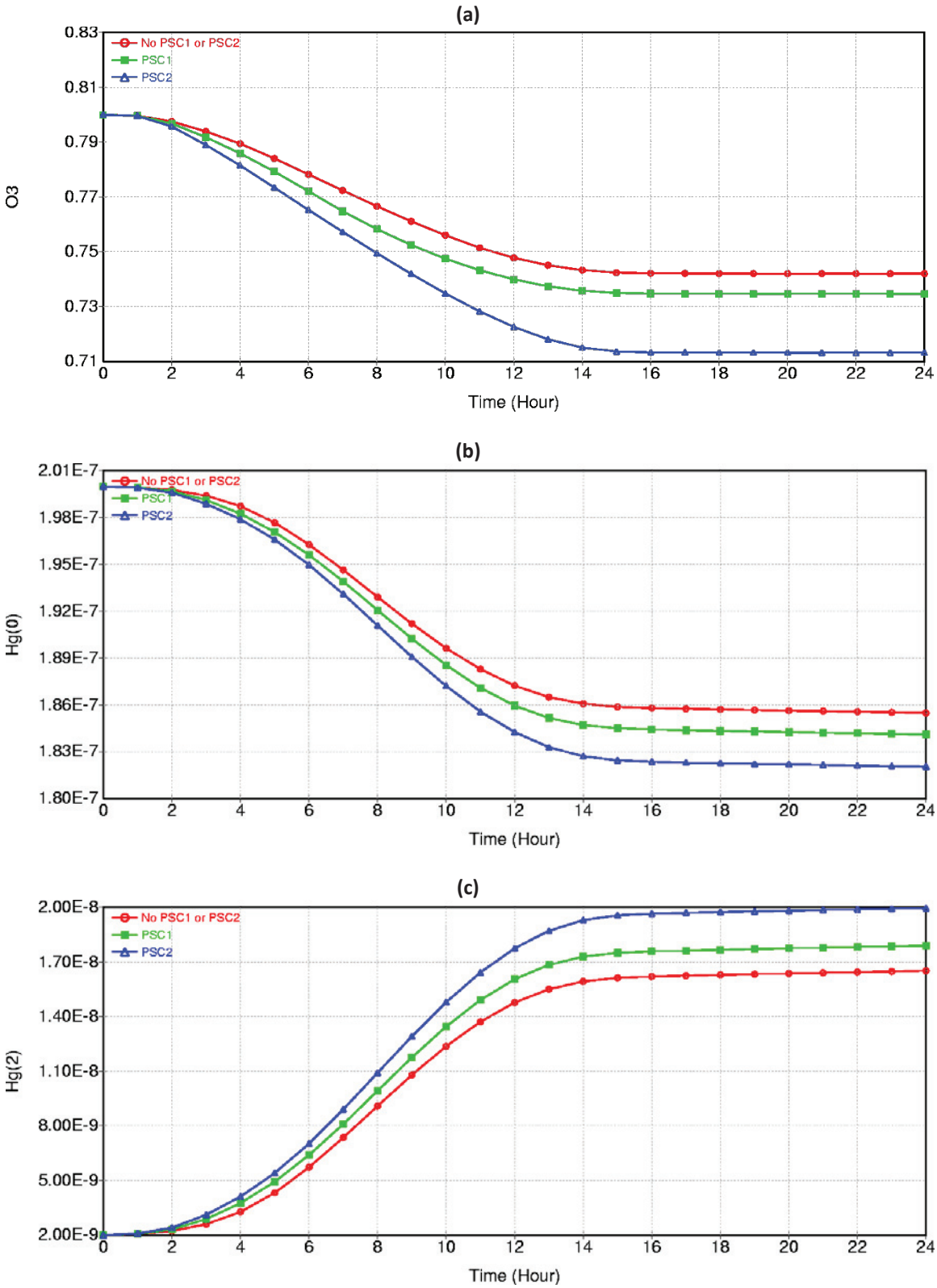

Figure 10. *Effects of Type I and Type II heterogeneous reactions on (a) O_3, (b) Hg(0) and (c) Hg(2) mixing ratios for a lower stratosphere scenario simulation. The red line represents the case with no PSC heterogeneous reactions, the green line represents the case with Type I PSC heterogeneous reactions, and the blue line represents the case with Type II PSC heterogeneous reactions.*

Table 7. *Hg(0) half-lives from the various oxidation pathways*

Oxidant	Half-life (hours)				
	Arctic Scenario		Upper Troposphere Scenario	Lower Stratosphere Scenario	
	With VOCs	Without VOCs		Type I PSCs	Type II PSCs
O_3	5 082	6 990	23 990	3 420	3 385
OH	83 990	41 990	8 187	345	327
H_2O_2	17 676	18 658	37 325	685 706	671 992
Br/BrO	366	19	293	576	446

4. Summary and Conclusions

We have incorporated several new reactions in the CB05 mechanism with chlorine extensions of Sarwar et al. (2006) to make the new mechanism (referred to as CB05_GE) suitable for use in global or global–through–urban scale applications. The new reactions in CB05_GE include the most important reactions needed for the lower stratosphere (< 30 km), such as the gas–phase reactions of odd hydrogen (HO_x), NO_x, ClO_x, and bromine oxides (BrO_x) and important reactions involving mercury species, as well as a number of heterogeneous reactions on aerosol particles, cloud droplets, and PSCs.

Zero–dimensional box model simulations conducted with CB05_GE for a variety of conditions illustrate the role of halogens such as chlorine and bromine on O_3 and mercury species. Heterogeneous chemistry also plays an important role in O_3 and mercury depletion events. The extent of ozone and mercury depletion in the box model simulations is lower than that observed during intense depletion episodes, partly due to the limitations of the box model in that it does not include dynamical processes such as mixing, and emissions from active halogen sources to replenish the reactive halogen species that are stabilized by reactions with carbonyl compounds such as formaldehyde. To overcome this limitation of the box model, sensitivity studies with very low initial hydrocarbon and formaldehyde concentrations are performed to achieve depletion levels comparable to observed events. Simulations for the lower stratosphere illustrate the importance of PSCs in providing a medium for the liberation of reactive halogens from the more stable forms of these species. Half–lives for Hg(0) oxidation calculated from sensitivity simulations with only one Hg(0) oxidation pathway activated show that, for most conditions, oxidation by Br and BrO is generally the most important pathway for Hg(0) depletion. However, the OH oxidation pathway is the fastest for the lower stratosphere scenarios.

The extended CB05_GE mechanism and the associated aerosol and aqueous–phase chemistry modules have been implemented into the unified Global–through–Urban Weather Research and Forecasting Model with Chemistry (GU–WRF/Chem), a three–dimensional coupled meteorological and air quality model that is being developed to simulate the interactions between global/regional climate change and regional/urban air pollution (Zhang et al., 2009a; Zhang et al., 2009b). Its implementation, application, and evaluation in GU–WRF/Chem will be presented in a future paper. This will be a comprehensive evaluation that will consider all aspects of the updates to the chemistry mechanism, including those not evaluated in this work, such as the performance of the mechanism for secondary organic aerosols (SOA).

Acknowledgments

This work was conducted under the U.S. EPA Science to Achieve Results (STAR) Program Grant # RD833376. We thank Dr. Golam Sarwar, U.S. EPA, for providing a box model version of CB05 as a starting point for our mechanism expansion and testing, and Mr. Shawn Roselle, U.S. EPA, for providing an early version of the CB05Cl mechanism. We also thank the anonymous reviewers and the APR editors for their invaluable suggestions in improving the manuscript.

References

Abbatt, J.P.D., Nowak, J.B., 1997. Heterogeneous interactions of HBr and HOCl with cold sulfuric acid solutions: implications for Arctic boundary layer bromine chemistry. *Journal of Physical Chemistry A* 101, 2131-2137.

Abbatt, J.P.D., 1994. Heterogeneous reaction of HOBr with HBr and HCl on ice surfaces at 228 K. *Geophysical Research Letters* 21, 665-668.

Archibald, A.T., Levine, J.G., Abraham, N.L., Cooke, M.C., Edwards, P.M., Heard, D.E., Jenkin, M.E., Karunaharan, A., Pike, R.C., Monks, P.S., Shallcross, D.E., Telford, P.J., Whalley, L.K., Pyle, J.A., 2011. Impacts of HO_x regeneration and recycling in the oxidation of isoprene: consequences for the composition of past, present and future atmospheres. *Geophysical Research Letters* 38, art. no. LO5804.

Archibald, A.T., Jenkin, M.E., Shallcross, D.E., 2010a. An isoprene mechanism intercomparison. *Atmospheric Environment* 44, 5356-5364.

Archibald, A.T., Cooke, M.C., Utembe, S.R., Shallcross, D.E., Derwent, R.G., Jenkin, M.E., 2010b. Impacts of mechanistic changes on HO_x formation and recycling in the oxidation of isoprene. Atmospheric Chemistry and Physics 10, 8097-8118.

Ariya, P.A., Dastoor, A.P., Amyot, M., Schroeder, W.H., Barrie, L., Anlauf, K., Raofie, F., Ryzhkov, A., Davignon, D., Lalonde, J., Steffen, A., 2004. The arctic: A sink for mercury. *Tellus Series B-Chemical and Physical Meteorology* 56, 397-403.

Ariya, P.A., Khalizov, A., Gidas, A., 2002. Reactions of gaseous mercury with atomic and molecular halogens: kinetics, product studies, and atmospheric implications. *Journal of Physical Chemistry A* 106, 7310-7320.

Ariya, P.A., Niki, H., Harris, G.W., Anlauf, K.G., Worthy, D.E.J., 1999. Polar sunrise experiment 1995: hydrocarbon measurements and tropospheric Cl and Br atoms chemistry. *Atmospheric Environment*, 33, 931-938

Bottenheim, J.W., Fuentes, J.D., Tarasick, D.W., Anlauf, K.G., 2002a. Ozone in the Arctic lower troposphere during winter and spring 2000 (ALERT2000). *Atmospheric Environment* 36, 2535-2544.

Bottenheim, J.W., Boudries, H., Brickell, P.C., Atlas, E., 2002b. Alkenes in the Arctic boundary layer at Alert, Nunavut, Canada. *Atmospheric Environment* 36, 2585-2594.

Boudries, H., Bottenheim, J.W., Guimbaud, C., Grannas, A.M., Shepson, P.B., Houdier, S., Perrier, S., Domine, F., 2002. Distribution and trends of oxygenated hydrocarbons in the high Arctic derived from measurements in the atmospheric boundary layer and interstitial snow air during the ALERT2000 field campaign. *Atmospheric Environment* 36, 2573–2583.

Bullock, O.R., Brehme, K.A., 2002. Atmospheric mercury simulation using the CMAQ model: formulation description and analysis of wet deposition results. *Atmospheric Environment* 36, 2135-2146.

Butler, T.M., Taraborrelli, D., Fischer, C.B.H., Harder, H., Martinez, M., Williams, J., Lawrence, M.G., Lelieveld, J., 2008. Improved simulation of isoprene oxidation chemistry with the ECHAM5/MESSy chemistry-climate model: lessons from the GABRIEL airborne field campaign. *Atmospheric Chemistry and Physics* 8, 4529-4546.

Calvert, J.G., Lindberg, S.E., 2005. Mechanisms of mercury removal by O_3 and OH in the atmosphere. *Atmospheric Environment* 39, 3355-3367.

Calvert, J.G., Lindberg, S.E., 2004a. Potential influence of iodine-containing compounds on the chemistry of the troposphere in the polar spring. I. Ozone depletion. *Atmospheric Environment* 38, 5087-5104.

Calvert, J.G., Lindberg, S.E., 2004b. The potential influence of iodine-containing compounds on the chemistry of the troposphere in the polar spring. II. Mercury depletion. *Atmospheric Environment* 38, 5105-5116.

Calvert, J.G., Lindberg, S.E., 2003. A modeling study of the mechanism of the halogen-ozone-mercury homogeneous reactions in the troposphere during the polar spring. *Atmospheric Environment* 37, 4467-4481.

Chang, C.T., Liu, T.H., Jeng, F.T., 2004. Atmospheric concentrations of the Cl atom, ClO radical, and HO radical in the coastal marine boundary layer. *Environmental Research* 94, 67-74.

Chen, S.A., Ren, X.R., Mao, J.Q., Chen, Z., Brune, W.H., Lefer, B., Rappengluck, B., Flynn, J., Olson, J., Crawford, J.H., 2010. A comparison of chemical mechanisms based on TRAMP-2006 field data. *Atmospheric Environment* 44, 4116-4125.

Davis, D., Crawford, J., Liu, S., McKeen, S., Bandy, A., Thornton, D., Rowland, F., Blake, D., 1996. Potential impact of iodine on tropospheric levels of ozone and other critical oxidants. *Journal of Geophysical Research-Atmospheres* 101, 2135-2147.

Dentener, F.J., Carmichael, G.R., Zhang, Y., Lelieveld, J., Crutzen, P.J., 1996. Role of mineral aerosol as a reactive surface in the global troposphere. *Journal of Geophysical Research-Atmospheres* 101, 22869-22889.

Dlugi, R., Berger, M., Zelger, M., Hofzumahaus, A., Siese, M., Holland, F., Wisthaler, A., Grabmer, W., Hansel, A., Koppmann, R., Kramm, G., Mollmann-Coers, M., Knaps, A., 2010. Turbulent exchange and segregation of HO_x radicals and volatile organic compounds above a deciduous forest. *Atmospheric Chemistry and Physics* 10, 6215-6235.

Ebinghaus, R., Kock, H.H., Temme, C., Einax, J.W., Lowe, A.G., Richter, A., Burrows, J.P., Schroeder, W.H., 2002. Antarctic springtime depletion of atmospheric mercury. *Environmental Science and Technology* 36, 1238-1244.

Emmerson, K.M., Evans, M.J., 2009. Comparison of tropospheric gas-phase chemistry schemes for use within global models. *Atmospheric Chemistry and Physics* 9, 1831-1845.

Eneroth, K., Holmen, K., Berg, T., Schmidbauer, N., Solberg, S., 2007. Springtime depletion of tropospheric ozone, gaseous elemental mercury and non-methane hydrocarbons in the European Arctic, and its relation to atmospheric transport. *Atmospheric Environment* 41, 8511-8526.

Engel, A., Muller, R., Schmidt, U., Carslaw, K.S., Stachnik, R.A., 2000. Indications of heterogeneous chlorine activation on moderately cold aerosol based on chlorine observations in the Arctic stratosphere. *Atmospheric Environment* 34, 4283-4289.

Fain, X., Obrist, D., Hallar, A.G., Mccubbin, I., Rahn, T., 2009. High levels of reactive gaseous mercury observed at a high elevation research laboratory in the Rocky Mountains. *Atmospheric Chemistry and Physics* 9, 8049-8060.

Fan, S.M., Jacob, D.J., 1992. Surface ozone depletion in Arctic spring sustained by bromine reactions on aerosols. *Nature* 359, 522-524.

Finlayson-Pitts, B.J., 2010. Halogens in the troposphere. *Analytical Chemistry* 82, 770-776.

Finlayson-Pitts, B.J., Pitts,J.N., 2000. *Chemistry of the Upper and Lower Atmosphere: Theory, Experiments, and Applications*, Academic Press, San Diego, CA, 970 pp.

Foster, K.L., Plastridge, R.A., Bottenheim, J.W., Shepson, P.B., Finlayson-Pitts, B.J., Spicer, C.W., 2001. The role of Br_2 and BrCl in surface ozone destruction at polar sunrise. *Science* 291, 471–474.

Friess, U., Deutschmann, T., Gilfedder, B.S., Weller, R., Platt, U., 2010. Iodine monoxide in the Antarctic snowpack. *Atmospheric Chemistry and Physics* 10, 2439-2456.

Friess, U., Hollwedel, J., Konig-Langlo, G., Wagner, T., Platt, U., 2004. Dynamics and chemistry of tropospheric bromine explosion events in the Antarctic coastal region. *Journal of Geophysical Research-Atmospheres* 109, art. no. D06305.

Gery, M.W., Whitten, G.Z., Killus, J.P., Dodge, M.C., 1989. A photochemical kinetics mechanism for urban and regional scale computer modeling. *Journal of Geophysical Research-Atmospheres* 94, 12925-12956.

Graedel, T.E., Keene, W.C., 1999. Preface. *Journal Of Geophysıcal Research* 104, 8331-8332.

Grannas, A.M., Shepson, P.B., Guimbaud, C., Sumner, A.L., Albert, M., Simpson, W., Domine, F., Boudries, H., Bottenheim, J., Beine, H.J., Honrath, R., Zhou, X.L., 2002. A study of photochemical and physical processes affecting carbonyl compounds in the Arctic atmospheric boundary layer. *Atmospheric Environment* 36, 2733-2742.

Grell, G.A., Peckham, S.E., Schmitz, R., McKeen, S.A., Frost, G., Skamarock, W.C., Eder, B., 2005. Fully coupled "online" chemistry within the WRF model. *Atmospheric Environment* 39, 6957-6975.

Hall, B., 1995. The gas-phase oxidation of elemental mercury by ozone. *Water Air and Soil Pollution* 80, 301-315.

Henze, D.K., Seinfeld, J.H., 2006. Global secondary organic aerosol from isoprene oxidation. *Geophysical Research Letters* 33, art. no. L09812.

Holmes, C.D., Jacob, D.J., Yang, X., 2006. Global lifetime of elemental mercury against oxidation by atomic bromine in the free troposphere. *Geophysical Research Letters* 33, art. no. L20808.

Honninger, G., Platt, U., 2002. Observations of BrO and its vertical distribution during surface ozone depletion at Alert. *Atmospheric Environment* 36, 2481-2489.

Hopper, J.F., Barrie, L.A., Silis, A., Hart, W., Gallant, A.J., Dryfhout, H., 1998. Ozone and meteorology during the 1994 Polar Sunrise Experiment. *Journal of Geophysical Research-Atmospheres* 103, 1481-1492.

Huang, R.J., Seitz, K., Buxmann, J., Pohler, D., Hornsby, K.E., Carpenter, L.J., Platt, U., Hoffmann, T., 2010. In situ measurements of molecular iodine in the marine boundary layer: the link to macroalgae and the implications for O_3, IO, OIO and NO_x. *Atmospheric Chemistry and Physics.*, 10, 4823-4833.

Huang, J.-P., X.-M. Hu, Y. Zhang, G. Sarwar, T.L. Otte, R. Gilliam, and K.L. Schere, 2006. Implementation and testing of the 2005 version of Carbon Bond Mechanism in WRF/Chem, presentation at the 7th Annual WRF User's Workshop, Boulder, CO, 19–22 June.

Huff, A.K., Abbatt, J.P.D., 2000. Gas-phase Br_2 production in heterogeneous reactions of Cl_2, HOCl, and BrCl with halide-ice surfaces. *The Journal of Physical Chemistry A* 104, 7284–7293.

IPCC, 2001. Climate Change 2001: The Scientific Basis. Contribution of Working Group I to the Third Assessment Report of the Intergovernmental Panel on Climate Change, Houghton, J.T.,Y. Ding, D.J. Griggs, M. Noguer, P.J. van der Linden, X. Dai, K., Maskell, and C.A. Johnson (editors), Cambridge University Press, Cambridge, United Kingdom and New York, NY, USA, 881pp.

Jacob, D.J., 2000. Heterogeneous chemistry and tropospheric ozone. *Atmospheric Environment* 34, 2131-2159.

Jacobson, M.Z., 2008. Effects of wind-powered hydrogen fuel cell vehicles on stratospheric ozone and global climate. *Geophysical Research Letters* 35, L19803, doi:10.1029/2008GL035102.

Jacobson, M.Z., 2005. *Fundamentals of Atmospheric Modeling, 2nd Edition*, Cambridge University Press, New York, NY.

Jacobson, M. Z, 2004. Climate response of fossil fuel and biofuel soot, accounting for soot's feedback to snow and sea ice albedo and emissivity. *Journal Of Geophysıcal Research* 109, art. no. D21201.

Jacobson, M.Z., 2001a. GATOR-GCMM: a global- through urban-scale air pollution and weather forecast model 1. Model design and treatment of subgrid soil, vegetation, roads, rooftops, water, sea ice, and snow. *Journal of Geophysical Research-Atmospheres* 106, 5385-5401.

Jacobson, M.Z., 2001b. GATOR-GCMM: 2. a study of daytime and nighttime ozone layers aloft, ozone in national parks, and weather during the SARMAP field campaign. *Journal of Geophysical Research-Atmospheres*

106, 5403-5420.

Jenkin, M.E., Watson, L.A., Utembe, S.R., Shallcross, D.E., 2008. A common representative intermediates (CRI) mechanism for VOC degradation. Part 1: gas phase mechanism development. *Atmospheric Environment* 42, 7185-7195.

Jockel, P., Tost, H., Pozzer, A., Bruhl, C., Buchholz, J., Ganzeveld, L., Hoor, P., Kerkweg, A., Lawrence, M.G., Sander, R., Steil, B., Stiller, G., Tanarhte, M., Taraborrelli, D., Van Aardenne, J., Lelieveld, J., 2006. The atmospheric chemistry general circulation model ECHAM5/MESSY1: consistent simulation of ozone from the surface to the mesosphere. *Atmospheric Chemistry and Physics* 6, 5067-5104.

Jockel, P., Sander, R., Kerkweg, A., Tost, H., Lelieveld, J., 2005. Technical note: the modular earth submodel system (MESSY) - a new approach towards earth system modeling. *Atmospheric Chemistry and Physics* 5, 433-444.

Karamchandani, P., Vijayaraghavan, K., Bronson, R., Chen, S.Y., Knipping, E.M., 2010. Development and application of a parallelized version of the advanced modeling system for transport, emissions, reactions and deposition of atmospheric matter (AMSTERDAM)-1. Model performance evaluation. *Atmospheric Pollution Research* 1, 271-279.

Keene, W.C., Khalil, M.A.K., Erickson, D.J., McCulloch, A., Graedel, T.E., Lobert, J.M., Aucott, M.L., Gong, S.L., Harper, D.B., Kleiman, G., Midgley, P., Moore, R.M., Seuzaret, C., Sturges, W.T., Benkovitz, C.M., Koropalov, V., Barrie, L.A., Li, Y.F., 1999. Composite global emissions of reactive chlorine from anthropogenic and natural sources: reactive chlorine emissions inventory. *Journal of Geophysical Research* 104, 8429-8440.

Kroll, J.H., Ng, N.L., Murphy, S.M., Flagan, R.C., Seinfeld, J.H., 2006. Secondary organic aerosol formation from isoprene photooxidation. *Environmental Science and Technology* 40, 1869-1877.

Kubistin, D., Harder, H., Martinez, M., Rudolf, M., Sander, R., Bozem, H., Eerdekens, G., Fischer, H., Gurk, C., Klupfel, T., Konigstedt, R., Parchatka, U., Schiller, C.L., Stickler, A., Taraborrelli, D., Williams, J., Lelieveld, J., 2010. Hydroxyl radicals in the tropical troposphere over the Suriname rainforest: comparison of measurements with the box model MECCA. *Atmospheric Chemistry and Physics* 10, 9705-9728.

Lary, D.J., Chipperfield, M.P., Toumi, R., Lenton, T., 1996. Heterogeneous atmospheric bromine chemistry. *Journal of Geophysical Research-Atmospheres* 101, 1489-1504.

Lehrer, E., Honninger, G., Platt, U., 2004. A one dimensional model study of the mechanism of halogen liberation and vertical transport in the polar troposphere. *Atmospheric Chemistry and Physics*, 4, 2427–2440.

Lelieveld, J., Butler, T.M., Crowley, J.N., Dillon, T.J., Fischer, H., Ganzeveld, L., Harder, H., Lawrence, M.G., Martinez, M., Taraborrelli, D., Williams, J., 2008. Atmospheric oxidation capacity sustained by a tropical forest. *Nature* 452, 737-740.

Li, S.M., 1994. Equilibrium of particle nitrite with gas-phase HONO: tropospheric measurements in the high Arctic during polar sunrise. *Journal of Geophysical Research-Atmospheres* 99, 25469-25478.

Lin, C.J., Pongprueksa, P., Lindberg, S.E., Pehkonen, S.O., Byun, D., Jang, C., 2006. Scientific uncertainties in atmospheric mercury models I: model science evaluation. *Atmospheric Environment* 40, 2911-2928.

Lindberg, S., Bullock, R., Ebinghaus, R., Engstrom, D., Feng, X.B., Fitzgerald, W., Pirrone, N., Prestbo, E., Seigneur, C., 2007. A synthesis of progress and uncertainties in attributing the sources of mercury in deposition. *Ambio* 36, 19-32.

Martinez, M., Harder, H., Kubistin, D., Rudolf, M., Bozem, H., Eerdekens, G., Fischer, H., Klupfel, T., Gurk, C., Konigstedt, R., Parchatka, U., Schiller, C.L., Stickler, A., Williams, J., Lelieveld, J., 2010. Hydroxyl radicals in the tropical troposphere over the Suriname rainforest: airborne measurements. *Atmospheric Chemistry and Physics* 10, 3759-3773.

Martinez, M., Arnold, T., Perner, D., 1999. The role of bromine and chlorine chemistry for Arctic ozone depletion events in NY-Alesund and comparison with model calculations. *Annales Geophysicae-Atmospheres Hydrospheres and Space Sciences* 17, 941-956.

Mason, R.P., Sheu, G.R., 2002. Role of the ocean in the global mercury cycle. *Global Biogeochemical Cycles* 16, art. no. 1093.

Morin, S., Honninger, G.H., Staebler, R.M., Bottenheim, J.W., 2005. A high time resolution study of boundary layer ozone chemistry and dynamics over the Arctic Ocean near Alert, Nunavut. *Geophysical Research Letters* 32, art. no. L08809.

Murphy, D.M., Hudson, P.K., Thomson, D.S., Sheridan, P.J., Wilson, J.C., 2006. Observations of mercury-containing aerosols. *Environmental Science and Technology* 40, 3163-3167.

Murphy, D.M., Thomson, D.S., 2000. Halogen ions and NO^+ in the mass spectra of aerosols in the upper troposphere and lower stratosphere. *Geophysical Research Letters* 27, 3217-3220.

Pal, B., Ariya, P.A., 2004. Gas-phase $HO^{\cdot}$-initiated reactions of elemental mercury: kinetics, product studies and atmospheric implications, *Environmental Science and Technology* 38, 5555-5566.

Pal, A., Ariya, P.A., 2003. Atmospheric reactions of gaseous mercury with ozone and hydroxyl radical: kinetics and product studies, *Journal de Physique IV*, 107, 189–192.

Pan, Y., X., Hu, M., Zhang, Y., 2008. Sensitivity of Gaseous and Aerosol Predictions to Gas-Phase Chemical Mechanisms, presentation at *the 10th Conference on Atmospheric Chemistry/the 88th AMS Annual Meeting*, New Orleans, LA, January 20–24.

Paulot, F., Crounse, J.D., Kjaergaard, H.G., Kurten, A., St Clair, J.M., Seinfeld, J.H., Wennberg, P.O., 2009. Unexpected epoxide formation in the gas-phase photooxidation of isoprene. *Science* 325, 730-733.

Peeters, J., Muller, J.F., 2010. HO_x radical regeneration in isoprene oxidation via peroxy radical isomerisations. II: experimental evidence and global impact. *Physical Chemistry Chemical Physics* 12, 14227-14235.

Peeters, J., Nguyen, T.L., Vereecken, L., 2009. HO_x radical regeneration in the oxidation of isoprene. *Physical Chemistry Chemical Physics* 11, 5935-5939.

Pohler, D., Vogel, L., Friess, U., Platt, U., 2010. Observation of halogen species in the Amundsen Gulf, Arctic, by active long-path differential optical absorption spectroscopy. *Proceedings of the National Academy of Sciences of the United States of America* 107, 6582-6587.

Pugh, T.A.M., MacKenzie, A.R., Hewitt, C.N., Langford, B., Edwards, P.M., Furneaux, K.L., Heard, D.E., Hopkins, J.R., Jones, C.E., Karunaharan, A., Lee, J., Mills, G., Misztal, P., Moller, S., Monks, P.S., Whalley, L.K., 2010a. Simulating atmospheric composition over a South-East Asian tropical rainforest: performance of a chemistry box model. *Atmospheric Chemistry and Physics* 10, 279-298.

Pugh, T.A.M., MacKenzie, A.R., Langford, B., Nemitz, E., Misztal, P.K., Hewitt, C.N., 2010b. The influence of small-scale variations in isoprene concentrations on atmospheric chemistry over a tropical rainforest. *Atmospheric Chemistry and Physics Discussion* 10, 18197-18234.

Pun, B.K., Seigneur, C., Michelsen, H., 2005a. *Chapter 12, Atmospheric transformations, in: Air Quality Modeling—Theories, Methodologies, Computational Techniques, and Available Databases and Software, Vol. II—Advanced Topics*, P. Zannetti (Editor), EnviroComp Institute and Air and Waste Management, Pittsburgh, PA.

Pun, B.K., C. Seigneur, J. Pankow, R. Griffin and E. Knipping, 2005b. An upgraded absorptive secondary organic aerosol partitioning module for three-dimensional air quality applications, *24th Annual American Association for Aerosol Research Conference*, Austin, Texas, 17-21 October.

Ramacher, B., Rudolph, J., Koppmann, R., 1999. Hydrocarbon measurements during tropospheric ozone depletion events: evidence for halogen atom chemistry. *Journal of Geophysical Research-Atmospheres* 104, 3633-3653.

Ramacher, B., Rudolph, J., Koppmann, R., 1997. Hydrocarbon measurements in the spring Arctic troposphere during the ARCTOC 95 campaign. *Tellus Series B-Chemical and Physical Meteorology* 49, 466-485.

Raofie, F. and P.A. Ariya, 2003. Kinetics and products study of the reaction of BrO radicals with gaseous mercury. *Journal de Physique Archives IV*, 107, 1119–1121.

Roselle, S.J., Luecken, D.J., Hutzell, W.T., Bullock, O.R., Sarwar, G. and Schere, K.L, 2007. Development of a multipollutant version of the Community Multiscale Air Quality (CMAQ) modeling system, presented at the *6th Annual CMAS Conference*, Chapel Hill, NC, October 1-3.

Ren, X.R., Olson, J.R., Crawford, J.H., Brune, W.H., Mao, J.Q., Long, R.B., Chen, Z., Chen, G., Avery, M.A., Sachse, G.W., Barrick, J.D., Diskin, G.S., Huey, L.G., Fried, A., Cohen, R.C., Heikes, B., Wennberg, P.O., Singh, H.B., Blake, D.R., Shetter, R.E., 2008. HO_x chemistry during intex-a 2004: observation, model calculation, and comparison with previous studies. *Journal of Geophysical Research-Atmospheres* 113, art. no. D05310.

Rotman, D.A., Atherton, C.S., Bergmann, D.J., Cameron-Smith, P.J., Chuang, C.C., Connell, P.S., Dignon, J.E., Franz, A., Grant, K.E., Kinnison, D.E., Molenkamp, C.R., Proctor, D.D., Tannahill, J.R., 2004. IMPACT, the LLNL 3-D global atmospheric chemical transport model for the combined troposphere and stratosphere: model description and analysis of ozone and other trace gases. *Journal of Geophysical Research-Atmospheres* 109, art. no. D04303.

Sander, S.P., Golden, D. M., Kurylo, M. J., Moortgat, G. K., Wine, P. H., Ravishankara, A. R., Kolb, C. E., Molina, M. J., Finlayson-Pitts, B. J., Huie, R. E., Orkin, V. L., Friedl, R. R., Keller-Rudek, H.,2006. *Chemical Kinetics and Photochemical Data for Use in Atmospheric Studies, Evaluation Number 15*, NASA/JPL Publication 06-2, Pasadena, CA.

Sarwar, G., Luecken, D., Yarwood, G., Whitten, G.Z., Carter, W.P.L., 2008. Impact of an updated carbon bond mechanism on predictions from the CMAQ modeling system: preliminary assessment. *Journal of Applied Meteorology and Climatology* 47, 3-14.

Sarwar, G., D.J. Luecken, and G. Yarwood, 2006. Developing And İmplementing An Updated Chlorine Chemistry İnto The Community Multiscale Air Quality Model, presented at the *28th NATO/CCMS International Technical Meeting*, Lepzig, Germany, May 15-19.

Schroeder, W.H., Anlauf, K.G., Barrie, L.A., Lu, J.Y., Steffen, A., Schneeberger, D.R., Berg, T., 1998. Arctic springtime depletion of mercury. *Nature* 394, 331-332.

Schroeder, W.H., Munthe, J., 1998. Atmospheric mercury - an overview. *Atmospheric Environment* 32, 809-822.

Schultz, M.G., L. Backman, Y. Balkanski, S. Bjoerndalsaeter, R. Brand, J.P. Burrows, S. Dalsoeren, M. de Vasconcelos, B. Grodtmann, D.A. Hauglustaine, A. Heil, J.J. Hoelzemann, I.S.A. Isaksen, J. Kaurola, W. Knorr, A. Ladstaetter-Weissenmayer, B. Mota, D. Oom, J. Pacyna, D. Panasiuk, J.M.C. Pereira, T. Pulles, J. Pyle, S. Rast, A. Richter, N. Savage, C. Schnadt, M. Schulz, A. Spessa, J. Staehelin, J.K. Sundet, S. Szopa, K. Thonicke, M. van het Bolscher, T. van Noije, P. van Velthoven, A.F. Vik, and F. Wittrock, 2007, *REanalysis of the TROpospheric Chemical Composition over the past 40 Years (RETRO) - A Long-Term Global Modeling Study of Tropospheric Chemistry*, Final Report, published as report no. 48/2007 in the series "Reports on Earth System Science" of the Max Planck Institute for Meteorology, Hamburg, ISSN 1614-1199, Jülich/Hamburg, Germany, August.

Seigneur, C., Lohman, K., 2008. Effect of bromine chemistry on the atmospheric mercury cycle. *Journal of Geophysical Research-Atmospheres* 113, D23309, doi:10.1029/2008JD010262.

Seigneur, C., Vijayaraghavan, K., Lohman, K., 2006. Atmospheric mercury chemistry: Sensitivity of global model simulations to chemical reactions. *Journal of Geophysical Research-Atmospheres* 111, art. no. D22306.

Seinfeld, J.H., Pandis, S.N., 1998. *Atmospheric Chemistry and Physics*, John Wiley & Sons, New York, NY.

Shibata, K., Deushi, M., Sekiyama, T.T., Yoshimura, H., 2005. Development of an MRI chemical transport model for the study of stratospheric chemistry, Papers in Meteorology and Geophysics, 55, 75–119.

Simpson, W.R., von Glasow, R., Riedel, K., Anderson, P., Ariya, P., Bottenheim, J., Burrows, J., Carpenter, L.J., Friess, U., Goodsite, M.E., Heard, D., Hutterli, M., Jacobi, H.W., Kaleschke, L., Neff, B., Plane, J., Platt, U., Richter, A., Roscoe, H., Sander, R., Shepson, P., Sodeau, J., Steffen, A., Wagner, T., Wolff, E., 2007. Halogens and their role in polar boundary-layer ozone depletion. *Atmospheric Chemistry and Physics* 7, 4375-4418.

Skov, H., Christensen, J.H., Goodsite, M.E., Heidam, N.Z., Jensen, B., Wahlin, P., Geernaert, G., 2004. Fate of elemental mercury in the Arctic during atmospheric mercury depletion episodes and the load of atmospheric mercury to the Arctic. *Environmental Science and Technology* 38, 2373-2382.

Sommar, J., Gardfeldt, K., Stromberg, D., Feng, X.B., 2001. A kinetic study of the gas-phase reaction between the hydroxyl radical and atomic mercury. *Atmospheric Environment* 35, 3049-3054.

Spicer, C.W., Plastridge, R.A., Foster, K.L., Finlayson-Pitts, B.J., Bottenheim, J.W., Grannas, A.M., Shepson, P.B., 2002. Molecular halogens before and during ozone depletion events in the Arctic at polar sunrise: concentrations and sources. *Atmospheric Environment* 36, 2721-2731.

Stavrakou, T., Peeters, J., Muller, J.F., 2010. Improved global modelling of HO_x recycling in isoprene oxidation: evaluation against the GABRIEL and INTEX-A aircraft campaign measurements. *Atmospheric Chemistry and Physics* 10, 9863-9878.

Steffen, A., Schroeder, W., Bottenheim, J., Narayan, J., Fuentes, J.D., 2002. Atmospheric mercury concentrations: measurements and profiles near snow and ice surfaces in the Canadian Arctic during alert 2000. *Atmospheric Environment* 36, 2653-2661.

Stockwell, W.R., Kirchner, F., Kuhn, M., Seefeld, S., 1997. A new mechanism for regional atmospheric chemistry modeling. *Journal of Geophysical Research-Atmospheres* 102, 25847-25879.

Stockwell, W.R., Middleton, P., Chang, J.S., Tang, X.Y., 1990. The 2nd generation regional acid deposition model chemical mechanism for regional air quality modeling. *Journal of Geophysical Research-Atmospheres* 95, 16343-16367.

Sumner, A.L., Shepson, P.B., Grannas, A.M., Bottenheim, J.W., Anlauf, K.G., Worthy, D., Schroeder, W.H., Steffen, A., Domine, F., Perrier, S., Houdier, S., 2002. Atmospheric chemistry of formaldehyde in the Arctic troposphere at polar sunrise, and the influence of the snowpack. *Atmospheric Environment* 36, 2553-2562.

Tarasick, D.W., Bottenheim, J.W., 2002. Surface ozone depletion episodes in the Arctic and Antarctic from historical ozonesonde records. *Atmospheric Chemistry and Physics* 2, 197-205.

Temme, C., Einax, J.W., Ebinghaus, R., Schroeder, W.H., 2003. Measurements of atmospheric mercury species at a coastal site in the Antarctic and over the South Atlantic Ocean during polar summer. *Environmental Science and Technology* 37, 22-31.

Tie, X.X., Brasseur, G., 1996. The importance of heterogeneous bromine chemistry in the lower stratosphere. *Geophysical Research Letters* 23, 2505-2508.

Tokos, J.J.S., Hall, B., Calhoun, J.A., Prestbo, E.M., 1998. Homogeneous gas-phase reaction of HgO with H_2O_2, O_3, CH_3I, and $(CH_3)_2S$: implications for atmospheric Hg cycling. *Atmospheric Environment* 32, 823-827.

Tuckermann, M., Ackermann, R., Golz, C., LorenzenSchmidt, H., Senne, T., Stutz, J., Trost, B., Unold, W., Platt, U., 1997. Doas-observation of halogen radical-catalysed Arctic boundary layer ozone destruction during the ARCTOC-campaigns 1995 and 1996 in Ny-Alesund, Spitsbergen. *Tellus Series B-Chemical and Physical Meteorology* 49, 533-555.

Utembe, S.R., Watson, L.A., Shallcross, D.E., Jenkin, M.E., 2009. A common representative intermediates (CRI) mechanism for VOC degradation. Part 3: development of a secondary organic aerosol module, *Atmospheric Environment* 43, 1982-1990.

Vogt, R., Sander, R., Von Glasow, R., Crutzen, P.J., 1999. Iodine chemistry and its role in halogen activation and ozone loss in the marine boundary layer: A model study. *Journal of Atmospheric Chemistry* 32, 375-395.

von Glasow, R., von Kuhlmann, R., Lawrence, M.G., Platt, U., Crutzen, P.J., 2004. Impact of reactive bromine chemistry in the troposphere. *Atmospheric Chemistry and Physics* 4, 2481-2497.

Watson, L.A., Shallcross, D.E., Utembe, S.R., Jenkin, M.E., 2008. A common representative intermediates (CRI) mechanism for VOC degradation. Part 2: gas phase mechanism reduction, *Atmospheric Environment* 42, 7196-7204.

Whalley, L.K., Edwards, P.M., Furneaux, K.L., Goddard, A., Ingham, T., Evans, M.J., Stone, D., Hopkins, J.R., Jones, C.E., Karunaharan, A., Lee, J.D., Lewis, A.C., Monks, P.S., Moller, S.J., Heard, D.E., 2011. Quantifying the magnitude of a missing hydroxyl radical source in a tropical rainforest. *Atmospheric Chemistry and Physics* 11, 7223-7233.

Yang, X., Cox, R.A., Warwick, N.J., Pyle, J.A., Carver, G.D., O'Connor, F.M., Savage, N.H., 2005. Tropospheric bromine chemistry and its impacts on ozone: a model study. *Journal of Geophysical Research-Atmospheres* 110, art. no. D23311.

Yarwood, G., S. Rao, M. Yocke, and G. Whitten, 2005. Updates to the Carbon Bond Chemical Mechanism: CB05, Final Report to the U.S. EPA, RT-04-00675, RTP, NC. http://www.camx.com/publ/pdfs/CB05_Final_Report_120805.pdf.

Zaveri, R.A., Peters, L.K., 1999. A new lumped structure photochemical mechanism for large-scale applications. *Journal of Geophysical Research-Atmospheres* 104, 30387-30415.

Zhang, H., Rattanavaraha, W., Zhou, Y., Bapat, J., Rosen, E.P., Sexton, K.G., Kamens, R.M., 2011. A new gas-phase condensed mechanism of Isoprene-NO_x photooxidation, *Atmospheric Environment* 45, 4507-4521.

Zhang, Y., Pan, Y., Wang, K., Fast, J.D., Grell, G.A., 2010. WRF/CHEM-MADRID: incorporation of an aerosol module into WRF/CHEM and its initial application to the TEXAQS2000 episode. *Journal of Geophysical Research-Atmospheres* 115, art. no. D18202.

Zhang Y., Pan, y., Wen, X.Y., Dong, X.Y., Karamchandani, P., Streets, D.G., Skamaroc, W.C., Grell, G.A., 2009a. Simulating climate-air quality interactions using global-through-urban WRF/Chem, presented at the *11th Conference on Atmospheric Chemistry/the 89th AMS Annual Meeting*, Phoenix, AZ, January 11-15.

Zhang, Y., Pan, Y., Wen, X.Y., Chen, Y.S., Karamchandani, P., Streets, D.G., Zhang, Q., 2009b. Global-through-urban WRF/Chem: a unified model for modeling aerosol-climate interactions, oral presentation at *The Goldschmidt 2009 Conference*, June 21-26, Davos, Switzerland.

Zhang, Y., Huang, J.P., Henze, D.K., Seinfeld, J.H., 2007. Role of isoprene in secondary organic aerosol formation on a regional scale. *Journal of Geophysical Research-Atmospheres* 112, art. no. D20207.

Zhang, Y., Pun, B., Vijayaraghavan, K., Wu, S.Y., Seigneur, C., Pandis, S.N., Jacobson, M.Z., Nenes, A., Seinfeld, J.H., 2004. Development and application of the model of aerosol dynamics, reaction, ionization, and dissolution (MADRID). *Journal of Geophysical Research-Atmospheres* 109, art. no. D01202.